International Journal of Earth Sciences
https://doi.org/10.1007/s00531-020-01951-4

ORIGINAL PAPER

Sequences, discontinuities and water stratification in a low-energy ramp: the Early Albian sedimentation in central Tunisia

Etienne Jaillard[1] · Abir Chihaoui[2] · Jean-Louis Latil[3] · Ihsen Zghal[4]

Received: 23 April 2020 / Accepted: 21 October 2020

Abstract

Based on a precise biostratigraphic framework stated previously, the detailed sedimentological study of eight sections of the early Albian succession of Central Tunisia made possible to refine the modalities of the Albian transgression and the related behavior of sedimentary system on the Tunisian margin. Major early Albian transgressive pulses occurred (i) at the base of the *L. tardefurcata* standard ammonite zone, (ii) around the top of the same zone, (iii) during the *D. mammillatum* standard zone, and (iv) near the top of the latter ammonite zone. They resulted in the progressive flooding of the Tunisian margin emergent since the Aptian boundary, in the disappearance of emergence evidences through time, in the southward backstepping of the carbonate shelf facies, and eventually in the homogeneization of the outer shelf marly sedimentation in the study area. The low energy of deposition of the early Albian sediments in this part of the South-Tethyan margin may be due to the deflection of winds and storms by the Coriolis forces toward the North-Tethyan margin, creating a clockwise gyre in this part of the ocean. This circulation may have enhanced upwelling currents likely responsible for phosphate mineralization, and for the oxygen depletion of deep waters, which progressively invaded the Tunisian margin, giving way to organic-rich deposits of late early Albian age. The early Albian sedimentation is then interrupted by a major hiatus of middle Albian to early late Albian age.

Keywords South tethyan margin · Sedimentology · Sequence stratigraphy · Marine transgression · Upwelling currents

Introduction

The Albian period is known for a long time, as the beginning of a widespread marine transgression of "Middle" Cretaceous age (e.g. Burollet 1956; Hancock and Kauffman 1979), classically related to intense volcanic activity and high spreading rates in oceans (Hays and Pitman 1973). The chronology and modalities of this sea-level rise, and its consequences on continental margins and on sedimentary systems, however, are still poorly constrained, mainly because most of shallow marine areas became emergent around the Aptian-Albian boundary, and because the early Albian deposits are usually made of monotonous marls. The Tunisian margin offers excellent outcropping conditions and highly fossiliferous sections, which allowed the establishment a detailed biostratigraphic framework of the Albian transgression in Central Tunisia (Dubourdieu 1956; Latil 2011). However, few detailed and comprehensive sedimentological studies are available so far on these series. This work aims at deciphering the stages and chronology of the jerky early Albian marine transgression, at highlighting the functioning of the Tunisian margin ramp during this transgression, and at evaluating the role of the paleogeographic setting of this part of the Tunisian margin on the genesis of discontinuities, phosphate formation and organic-rich deposits.

✉ Etienne Jaillard
Etienne.Jaillard@univ-grenoble-alpes.fr

1 IRD, Université Grenoble Alpes, ISTerre, CNRS, IFSTTAR, USMB, CS 40700, 38058 Grenoble Cedex 9, France

2 Université de Gabès, Rue Omar Ibn Khattab, 6029 Gabès, Tunisia

3 G.R.E.G.B., Le Maupas, 05300 Lazer, France

4 Université de Sfax, Route de l'Aéroport Km 0.5, BP 1169, 3029 Sfax, Tunisia

Published online: 06 November 2020

Geological setting and previous works

During Cretaceous times, Tunisia is part of the southern passive margin of the Tethys. There, Tethyan deposits began with transgressive, unconformable Triassic deposits overlain by Jurassic limestones, deposited in an extensional tectonic setting (Castany 1951; Busson 1972; Bouaziz et al. 2002; Bahrouni et al. 2015; Tlig 2015). During the Cretaceous, the Tunisian margin comprises three main paleogeographic domains (Zghal and Arnaud-Vanneau 2005; Soua 2015) (Fig. 1). To the South, the Saharan platform received a reduced, mainly continental to very shallow marine sedimentation, which is virtually undeformed according to current literature (e.g. Raulin et al. 2011; Gabtni et al. 2012; Krimi et al. 2017). Central Tunisia was marked by shallow marine, siliciclastic then calcareous deposits (e.g. Burollet 1956; M'Rabet 1995; Robaszynski et al. 2000; Ben Chaabane et al. 2019). It was separated from the Saharan platform by the Chott depression (Fig. 1) and is presently deformed by Cretaceous diapirs and E–W to NE-trending Alpine folds (Tunisian Atlas) (e.g. Zouaghi et al. 2005; Gharbi et al. 2015). The North Tunisian basin (Fig. 1) received thick marly deposits during most of the Cretaceous (Souquet et al. 1997; Burollet et al. 1983), and is presently marked by numerous NE–SW trending folds and thrusts, and by pinched diapirs (Tunisian Tell; Bobier et al. 1991; Masrouhi et al. 2014).

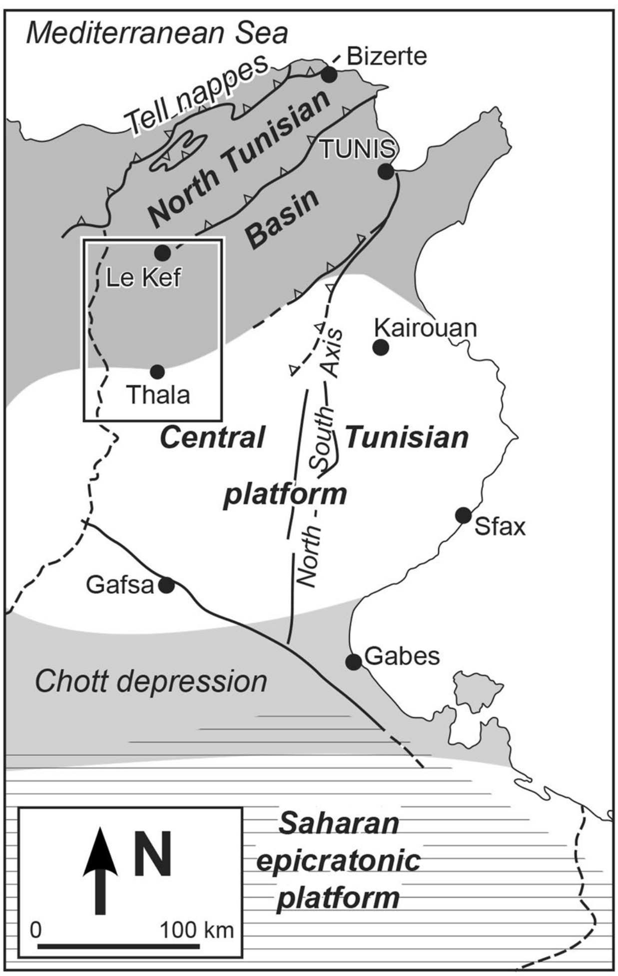

Fig. 1 Structural and paleogeographic sketch of Tunisia, and location of the study area

The Aptian-Cenomanian succession in northern Central Tunisia comprises from base to top (Burollet 1956): (1) the Serdj Formation (Fm) made of carbonate shelf deposits (Tlatli 1980; Lehmann et al. 2009; Heldt et al. 2010; Ben Chaabane et al. 2019), (2) the Hameima Fm that includes marl, sandstone and limestone beds of shallow marine environment (Chihaoui 2009; Ben Chaabane et al. 2019), and (3) the poorly studied, thick and monotonous Fahdene Fm, mostly made of argillaceous marls, with some limestone beds (Burollet 1956; Chihaoui et al. 2010) (Fig. 2). Burollet (1956) subdivided the Fahdene Fm into a basal Ammonite-rich horizon, the Lower Shales, the Allam limestones, the Middle Shales and the Upper Shales (Fig. 2). The two latter subunits, of late Albian and Cenomanian age, respectively, are out of the scope of this study.

Since the pioneer work by Burollet (1956), Dubourdieu (1956) and M'Rabet (1981), the stratigraphy and sedimentology of the Hameima Fm and its equivalents have been studied by Chihaoui (2009), Chihaoui et al. (2010) and Ben Chaabane et al. (2019), based on the ammonite biostratigraphic framework by Latil (2011). The Lower Fahdene Fm and its equivalent have been mainly studied for biostratigraphic purposes (Vila et al. 1995; Zghal et al. 1997; Chihaoui et al. 2010; Latil 2011; Ben Fadhel et al. 2014), for potential source-rocks analyses (Khalifa et al. 2018; Talbi et al. 2019) or for synsedimentary tectonics (e.g. Martinez et al. 1991; Arfaoui et al. 2011; Jaillard et al. 2013; 2017; Masrouhi et al. 2014). Finally, some publications deal with the sedimentology of the latest Albian to Cenomanian deposits (Robaszynski et al. 1993; 2008; Jaillard et al. 2005; Layeb et al. 2012).

The stratigraphic location of the Aptian-Albian boundary in Tunisia has been long debated. Works by Chihaoui et al. (2010) and Latil (2011) established that the Aptian-Albian boundary, as defined by ammonites, corresponds to the base of a marked marine transgression, recorded at the base of the Hameima Fm in the Tajerouine area (Chihaoui et al. 2010). Note that this definition does not coincide with the Aptian-Albian boundary defined by Kennedy et al. (2000; 2017) on the base of microfossils. Using the latter, Ben Chaabane et al. (2019) placed the Aptian-Albian boundary in the upper part of the Serdj Fm in NE Tunisia.

Farther Southeast, early to middle Albian times are marked by an emergence period (Burollet 1956; Bismuth et al. 1981; Philip et al. 1989; Touir et al. 2015). However,

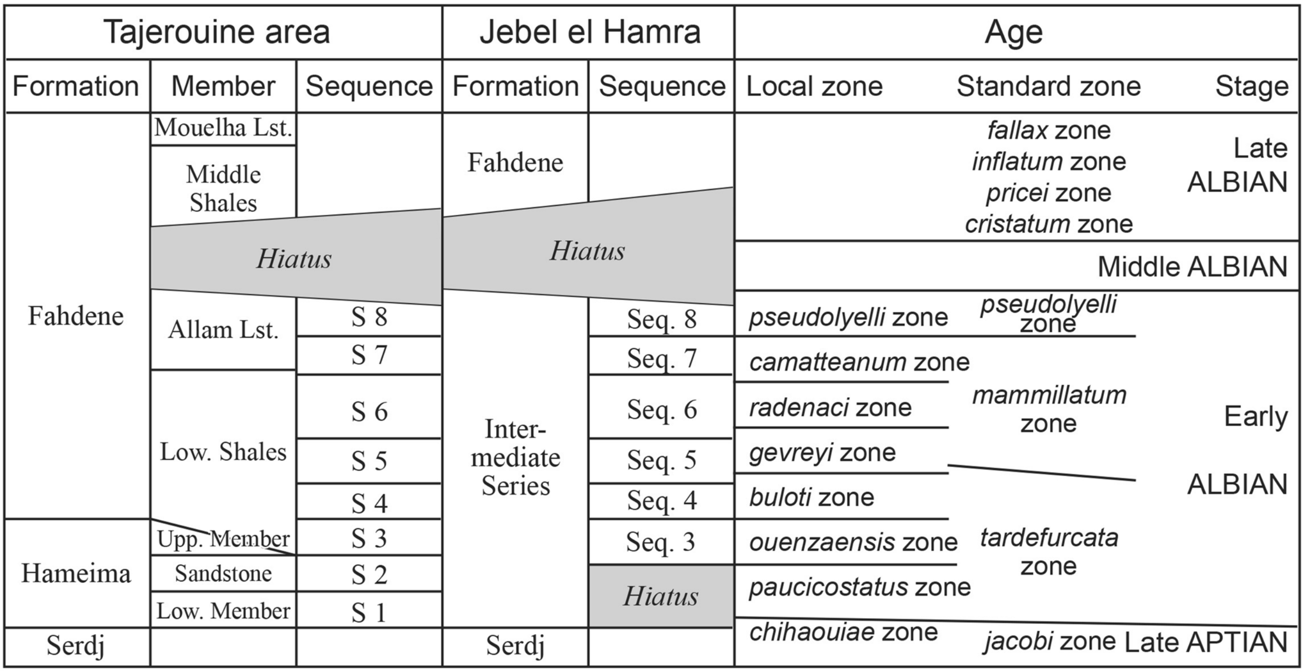

Fig. 2 Litho- and bio-stratigraphic framework (ammonite zones) of the studied sedimentary units, after from Burollet (1956), Chihaoui et al. (2010) and Latil (2011)

the early Albian transgression had been recently identified in some sites of central Tunisia (Kebar Fm: Trabelsi et al. 2010; Salmouna et al. 2017; Houla et al. 2017), and in Jebel el Hamra. In the latter location, El Euchi (1993) identified the "Intermediate Series", now dated as early Albian (Latil 2011) (Fig. 2), which is overlain by the Middle and Upper Shales of the Fahdene Fm, of late Albian and Cenomanian age, respectively (Jaillard et al. 2013).

Materials and methods

Here, we present the detailed sedimentological study of several sections. In the Tajerouine area (NW Tunisia), we studied four sections of the Hameima Fm and lower part of the Fahdene Fm (Fig. 3). The El Goussa section has been studied 7.5 km WNW of Jebel Hameima (Lower Shales), and 3.8 km farther NNE (7.2 km NNW of Jebel Slata) along the road to Tajerouine (Allam Limestones). The Hameima section corresponds to the 2.5 km long, nice outcrops located North of Jebel Hameima (see Zghal et al. 1997). The Slata section has been measured north of the northern tip of Jebel Slata (Charrens section of Chihaoui 2009) and completed by numerous punctual observations (Jaillard et al. 2017). In the Jerissa section, the Hameima Fm has been studied on the western flank of the secondary hill located South of the main jebel, and the Allam Limestone was measured 1.5 km farther Eest (southeast of Jebel Jerissa). The Bou el Haneche section has been studied on the southern flank of Jebel Bou el Haneche (Hameima Fm) and across the 2 km long outcrop located West of Jebel Bou el Haneche (Fahdene Fm) (Fig. 3).

In Jebel el Hamra, five sections have been studied along its southwestern flank. The northernmost section was measured immediately south of the hamlet located south of the road to Tebessa (Algeria). The southernmost section has been studied at the southwestern tip of the jebel. Three short sections have been studied between the two latter, among which one is presented here (Fig. 3).

The Hameima Fm has been studied through field observations of the lithology, sedimentary structures and faunal content, and through thin-section analysis with optical microscope (details in Chihaoui 2009). Because of its mainly argillaceous lithology, the Fahdene formation has been mainly studied through field observations, completed with scarce thin-section analysis.

Depositional sequences are defined and described following the definitions of Van Wagoner et al. (1988; Emery and Myers 1996). They comprise a Lowstand Systems Tract (LST), often missing, a Transgressive Systems Tract (TST), and a Highstand Systems Tract (HST), and will be called Sequence 1 to 9, or S1 to S9. Depositional sequences are defined by significant sedimentary discontinuities assumed to be sequences boundaries, labelled D1 to D10. The described sequences are tentatively considered

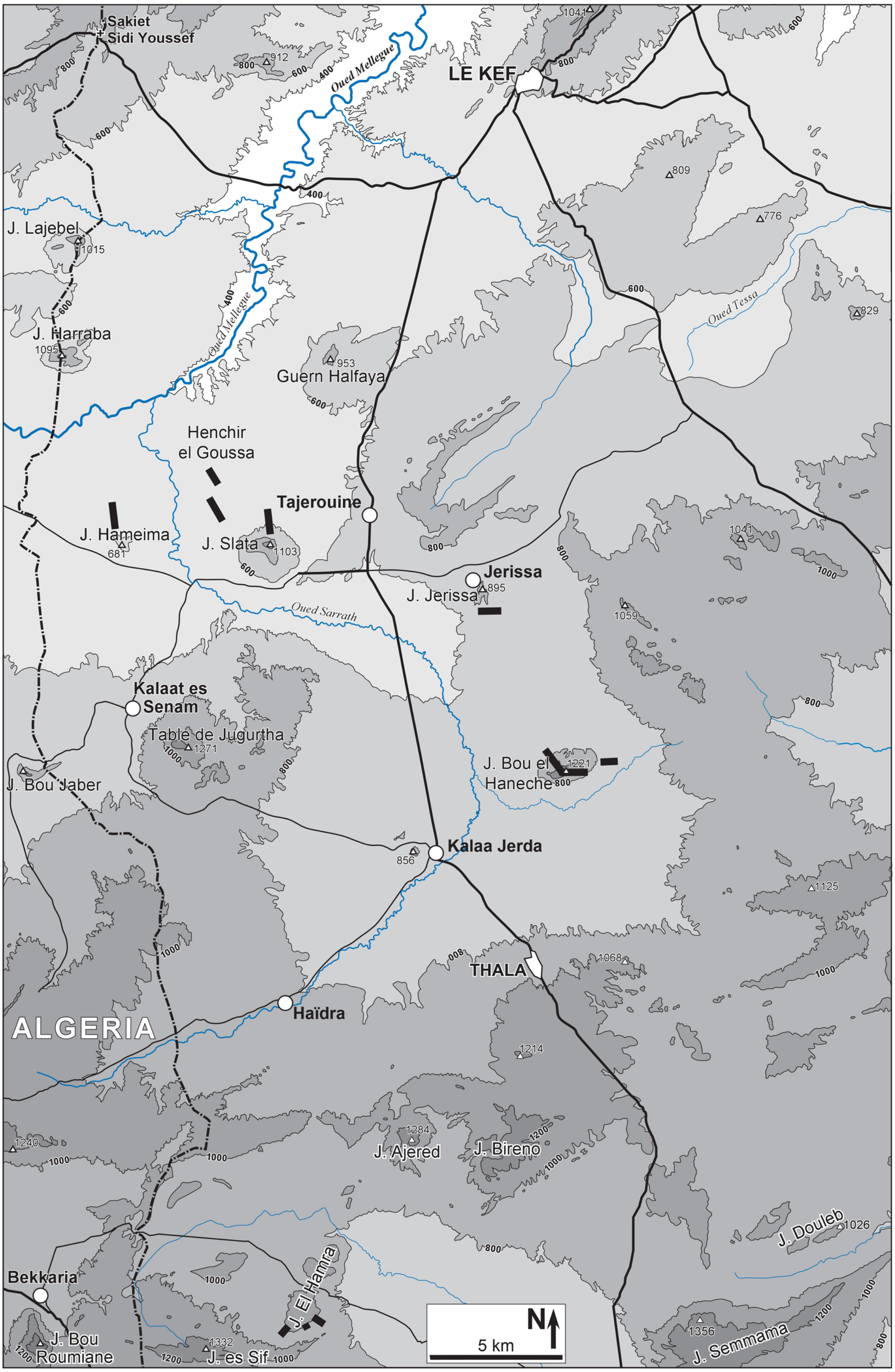

Fig. 3 Sketchy map of the study area. Location of sections is indicated by thick bars

3rd order depositional sequences (Haq 2014), which may be constituted by minor sequences.

We followed the stratigraphic framework established by Burollet (1956), later refined by Chihaoui et al. (2010) (Fig. 2). Stratigraphic ages are those proposed by Latil (2011).

Sedimentology

Early Albian transgression in the Tajerouine area

Mixed clastic-carbonate shelf (Hameima Fm, earliest Albian)

The Hameima Formation overlies the massive limestone and dolomites of the Serdj Fm (Heldt et al. 2010; Ben Chaabane et al. 2019) and can be subdivided into two depositional sequences (S1 and S2 on Fig. 4; Chihaoui 2009). These sequences are of earliest Albian age (*H. paucicostatus* local ammonite zone, lower part of the *L. tardefurcata* standard ammonite zone), except may be for the unfossiliferous very base of the formation (Latil 2011).

The first sequence comprises four minor sequences (1a to 1d, Fig. 4), showing a rather homogeneous facies succession, from base to top (Fig. 4):

A. Bioturbated marls with scarce calcareous beds, scarce ammonites, thick bivalve shells, crinoids, irregular and regular urchins, gastropods and scarce ostreids. Both the lithology and the faunal content suggest an open marine shelf environment.

B. Alternating marls and bioturbated limestone layers, with large bivalves, pectinids, irregular urchins, scarce crinoids, pinnidae, trigonids and scarce brachiopods. These features point to a shallow marine shelf environment.

C. Limestone beds separated by thin marl interbeds, with abundant orbitolinids, bioclasts, regular urchins, oysters, and locally rudistids, oolites. The uppermost massive limestone bed is capped by a karstified surface, infilled with overlying deposits. These are interpreted as deposited in a very shallow carbonate shelf environment.

In minor sequences 1a and 1d, only facies B and C of the succession are present (Fig. 4), expressing an overall shallow marine deposition environment. In minor sequence 1b, facies A and B can be recognized, thus expressing a deeper depositional setting than sequences 1a and 1d. The deepest depositional environment is, thus, regarded as occurring during sequence 1b, representing the Maximum Flooding period of S1. In the Hameima and Jerissa sections, thin sandstone beds are present, either in the retrograding (thinning upward) series (base of sequence 1b) or in the prograding (thickening upward) part of the minor sequences (sequence 1c, Fig. 4).

The 2nd sequence is marked by the abundance of sandstone layers and comprises three minor sequences (Fig. 4). The first minor sequence (2a, Fig. 4) begins with marls and ends up with a massive sandstone bed displaying sedimentary structures and fossil content of very shallow marine environment (current ripples, Hummocky Cross Stratification (HCS), orbitolinids, wood fragments). The second minor sequence (2b, Fig. 4) is mainly made of fine-grained, very well-sorted sandstones with little matrix. They are marked by shallow-water energy features at the base (horizontal laminae, HCS, current ripples), marly or calcareous intercalations in their middle part, and massive beds of sandstone or orbitolinid-rich sandy limestone at the top. This succession is regarded as a first retrograding, then prograding succession. This interpretation is supported by the faunal content. The latter includes scarce orbitolinids, ostreids and plant remnants at the base, large bivalves, echinoids and scarce ammonites in the middle part, and ostreids, annelids and orbitolinids in the upper part. The third minor sequence (sequence 2c, Fig. 4) is mainly made of an orbitolinid-rich limestone series, the top of which is deeply karstified (Fig. 4). In most sections, the fauna and sedimentary structures (corals, trigonids, ostreids, algae, oncolites, peloids) evidence a very shallow marine deposition for sequence 2c. In the Hameima section, however, this sequence is represented by ammonite-bearing marl and sandstones. There, although ammonites are common, the presence of pinnidae, trigonids and ostreids, as well as current ripples, HCS and planar laminae, indicates a shallow marine depositional environment.

Transition from carbonate shelf to muddy ramp (Hameima to Fahdene Fm)

The transition from the mainly calcareous and sandy Hameima Fm (mixed carbonate shelf system) to the mainly marly Fahdene Fm (shaly ramp system) occurs within the transition from the *H. paucicostatus* to the *H. buloti* ammonite zones (*L. tardefurcata* standard ammonite zone) (Figs. 2 and 4). It occurs at the top of the sandstone beds (sequence 2b) in the northwestern Hameima section, whereas orbitolinid-rich limestone (Sequence 3) is still recorded at the top of the *M. ouenzaensis* zone in the Jerissa and Bou el Haneche sections located farther Southeast. In the Jerissa section, massive limestone beds seem to be still present within the *H. buloti* zone, but the succession is disturbed by numerous minor faults that make uncertain the observed succession. Since the Jerissa and Bou el Haneche section are located to the SE, the later disappearance of the shelf limestone in these places is interpreted as resulting from the southeastward retrogradation of the carbonate platform during the early Albian eustatic rise.

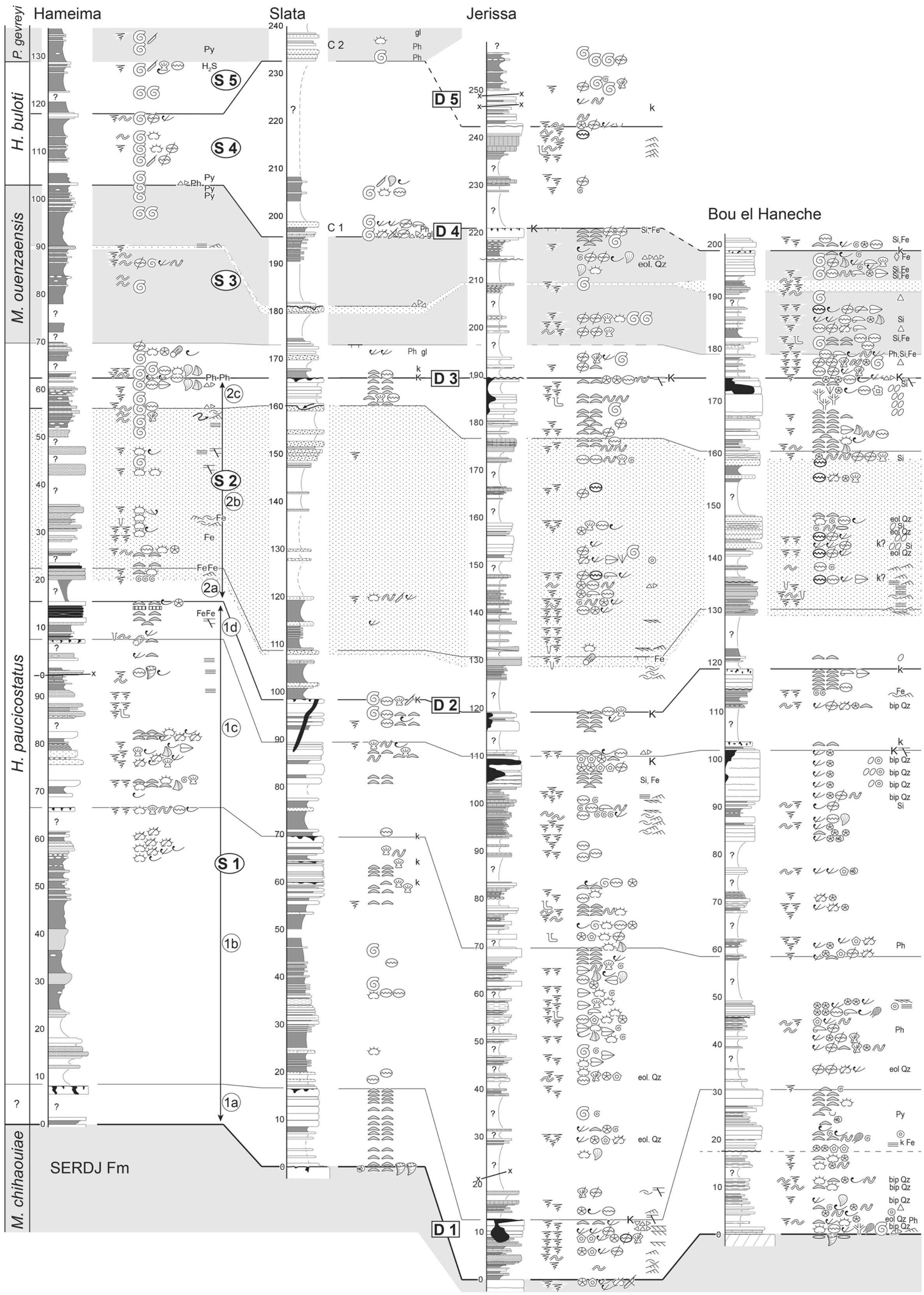

Fig. 4 Sections of the Hameima Fm and base of the Fahdene Formation in the Tajerouine area: lithology, sedimentary features and correlations. Grey area: ammonite zones (time equivalence). Dotted area: sandy interval. Location on Fig. 3. Caption on Fig. 5

This transitional series is interpreted as representing a third depositional sequence (S3 on Fig. 4). As a matter of fact, in the southeastern sections, its base is marked by shallow marine benthic bivalves (trigonids, pinnidae, ostreids) and orbitolinids, associated with scarce ammonites. The middle part of the succession is mainly marly and contains deeper benthic fauna (annelids, brachiopods, large bivalves, ostreids, other bivalves) and some ammonites (Maximum Flooding Interval). The upper part is marked in the southeastern sections by orbitolinid-rich limestone beds that also host ostreids, trigonids, regular urchins and scarce brachiopods, and the top of which is karstified.

Farther South, in Jebel Ajered (location on Fig. 3), 30–50 m of massive limestone bearing orbitolinids, rudistids and corals, rest on the Serdj Fm. They are overlain by alternating marl and limestone beds (Fahdene Fm, Lower Shales), and then by a series of dark limestone (Allam Limestone) (Burollet 1956). The ammonite *M. jaillardi* (top of *M. ouenzaensis* zone; Latil 2011) has been found a few meters below the top of the massive limestones. This indicates that the end of the shallow carbonate shelf deposition, comparable to that of the Serdj Fm, occurred there later than in the Hameima area and was coeval with that recorded in the Slata, Jerissa and Bou el Haneche sections. This confirms the retrogradation of the carbonate shelf deposits during the early Albian marine transgression (Chihaoui et al. 2010; Ben Chaabane et al. 2019).

Muddy Ramp (Fahdene Fm)

Overlying the transitional sequence (S3) described above, the lower part of the Fahdene Fm comprises five identified depositional sequences of early Albian age (Fig. 5). The three first sequences correspond to the Lower Shales (Chihaoui et al. 2010), while the two upper sequences represent the Allam Limestone (Burollet 1956; Chihaoui et al. 2010).

In the Lower Shales, the base of each sequence (Figs. 5, S4–S6) is an erosional surface located at the base of a calcareous bed. The latter is 10–50 cm thick, may be lens-shaped and contains reworked calcareous clasts at the base. It locally shows abundant bivalves and ammonites, or may be azoic. The reworked clasts are micritic and their outer surface is phosphatized (already described by Dubourdieu (1956)). In the northwestern sections, the basal calcareous bed is lacking, and the discontinuity is only marked by a thin sandy level and/or by reworked ammonites.

In most sections, the basal limestone bed is overlain by alternating marly limestone beds and clayey marl. This succession contains an abundant benthic fauna comprising brachiopods, abundant irregular urchins, annelids, gastropods, some ostreids, plicatulids and other bivalves, associated with belemnites and ammonites, and is usually highly bioturbated. This association indicates an open marine, middle ramp depositional setting. In the Slata section, the base of the sequences is made of coarse-grained, phosphate-rich calcarenite beds (C1 to C3, Fig. 5), suggesting a high-energy environment. This, associated with sea urchins, brachiopods, ammonites, belemnites and abundant bivalve fragments of outer shelf environment, suggests deposition on a swell.

In all sections, the middle part of the sequences is composed of clayey marl rich in pyrite with few thin beds of bioturbated limestone, almost devoid of benthic fauna. Few ammonites and belemnites are associated with scarce gastropods and irregular urchins, and may be replaced by pyrite. This faunal association indicates a rather deep, outer ramp environment (Maximum Flooding period). The scarcity of the benthic fauna and the abundance of pyrite suggest an oxygen-depleted environment.

Locally, the upper part of the sequences shows calcareous beds containing belemnites, plicatulids, annelids and pinnidae, which suggest a shallowing upward trend. In other sites, the erosional surface and the subsequent phosphatized clast-bearing limestone bed directly overlie the argillaceous part of the sequence. In all cases, large-sized calcareous nodular concretions are common in the uppermost part of the sequences, the core of which presents radial fractures infilled with calcite (septaria).

In the Allam Limestone (S7 and S8, Fig. 5), the sequences are monotonous and almost devoid of fauna. The base of the sequences is marked by a thinning-upward alternation of dark clayey marl and thin beds of black limestone that contain scarce belemnites and very rare ammonites. In the Slata section, the base of S7 is represented by beds of phosphate-rich calcarenite (C4 on Fig. 5), and the lower part of S7 is rich in phosphate and glauconite, suggesting a high-energy and relatively condensed sedimentation (see below).

The middle parts of the sequences are mainly argillaceous, almost azoic, and are overlain by a thickening-upward alternation of clayey marl and micritic limestone that constitutes the upper parts of the sequences. The uppermost part of S8 is commonly silicified. Very scarce benthic fauna occurs mainly in the lowermost or uppermost parts of the sequences, and is represented by scarce buchidae (*Aucellina* sp.) and inoceramid bivalves (Fig. 5). This faunal association (e.g. Henderson 2004), together with the abundance of pyrite and the lack, or scarcity of bioturbation points to a dysaerobic environment. Farther North, deposits correlated with the Allam limestones (S7 and S8) are considered potential source-rocks (Ben Fadhel et al. 2011, 2014). Very scarce ammonites allowed to ascribe S7 to the *T. camatteanum* zone, and S8 to the *L. pseudolyelli* zone (Latil 2011). The top of S8, however, is barren of ammonites, and may be either of early middle Albian age, or more probably, of late early Albian age (Latil 2011). Lithological correlations suggest the presence of minor sequences within S7 and S8 (7a, 7b, 8a, 8b in Fig. 5), but clear discontinuities have not

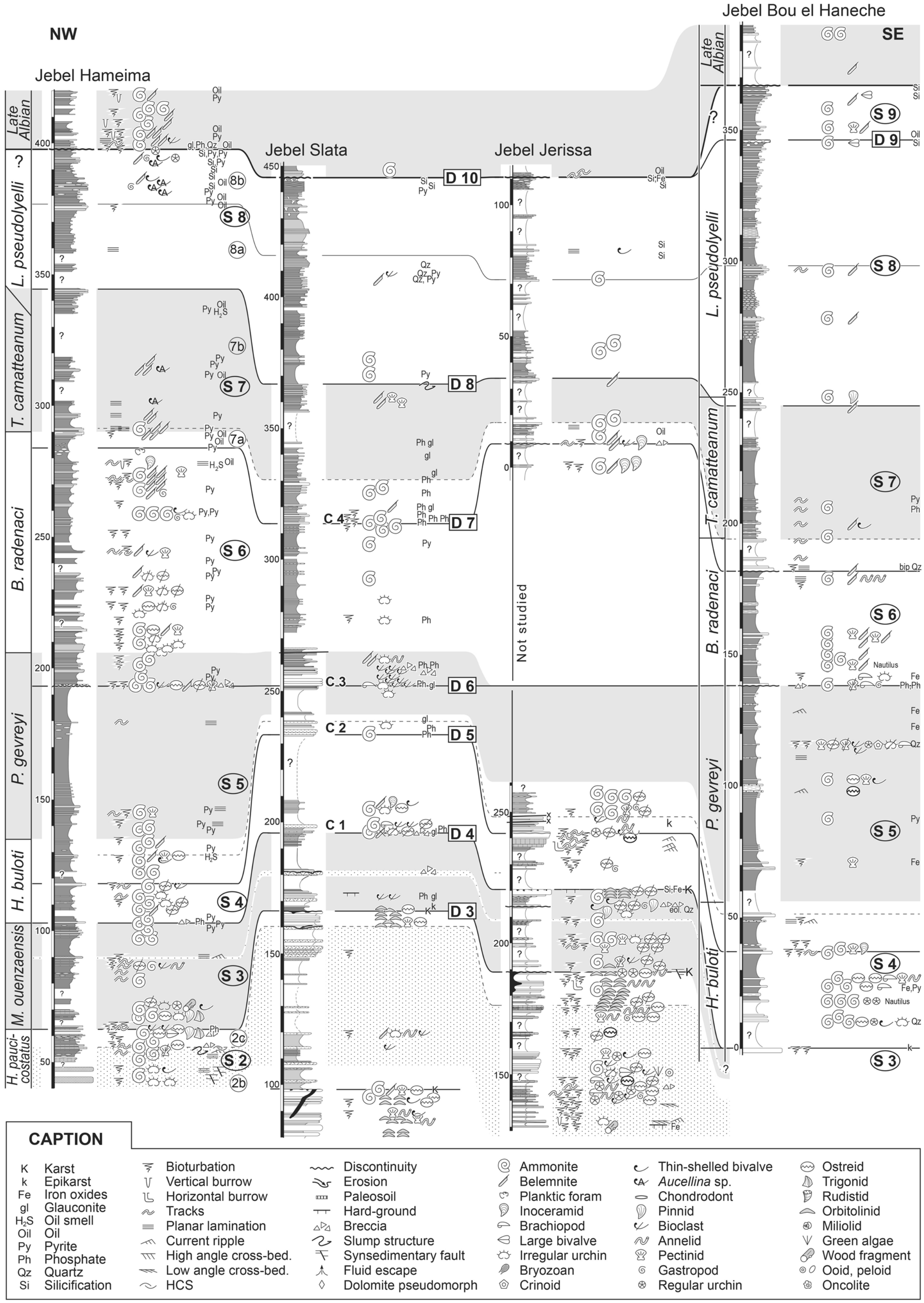

Fig. 5 Sections of the Fahdene Formation in the Tajerouine area: lithology, sedimentary features and correlations. Shaded areas: ammonite zones; Dotted area: Sandy unit of S2. Location on Fig. 3

been identified in the field. In the Bou el Haneche section, an additional sequence can be observed. However, poorly preserved ammonites did not allow to date this unit (Latil 2011). Since it is overlain by a major discontinuity (silicified erosional surface), it probably belongs to the Allam Limestone, and may be either of latest early Albian, or of early middle Albian age (S9 in Fig. 5).

The top of the S8 sequence (and S9 where present) is a major discontinuity that contains at least most of the middle Albian and part of the late Albian time span (Chihaoui et al. 2010). In most sections, it is an uneven, corroded, silicified surface, locally blanketed by fine-grained, well-sorted sandstone, locally bearing oil (Hameima). Silicification affected the underlying strata to a depth of 10 to 15 m thick to the Northwest (El Goussa), and of 5 m to the Southeast (Bou el Haneche).

Early Albian transgression in Jebel El Hamra

In Jebel El Hamra, the Lower Albian succession ("Intermediate Series" of El Euchi 1993) can be divided into six depositional sequences (S3 to S8, Fig. 6), which can be correlated with the sequences of the Tajerouine area (Latil 2011) (Fig. 2).

Sequences 3 to 5 are made of a basal marly interval, capped by a dolomitic bed, the top of which is deeply karstified. The marly part of the sequences contains scarce benthic fauna (irregular sea urchins, pectinids, gastropods, ostreids) associated with scarce ammonites. In some cases, intermediate beds occur, that can be correlated from a section to another. The first sequence (S3, Fig. 6) only yielded a *Parengonoceras* sp. that suggests an early Albian age. Since S4 and S5 are ascribed to the *"H". buloti* and *P. gevreyi* ammonite zones, respectively (Latil 2011), S3 of El Hamra is tentatively correlated with S3 of the Tajerouine area (*M. ouenzaensis* ammonite zone; Fig. 4).

Sequence 6 is well developed in the southern part of the jebel, is much thinner in the intermediate section, and is represented to the Northeast, by a thin phosphate-rich sandy level containing ostreids, pectinids and other bivalves (Fig. 6). Because S3 to S5 shows comparable thicknesses in all sections, jebel El Hamra is likely to have undergone a

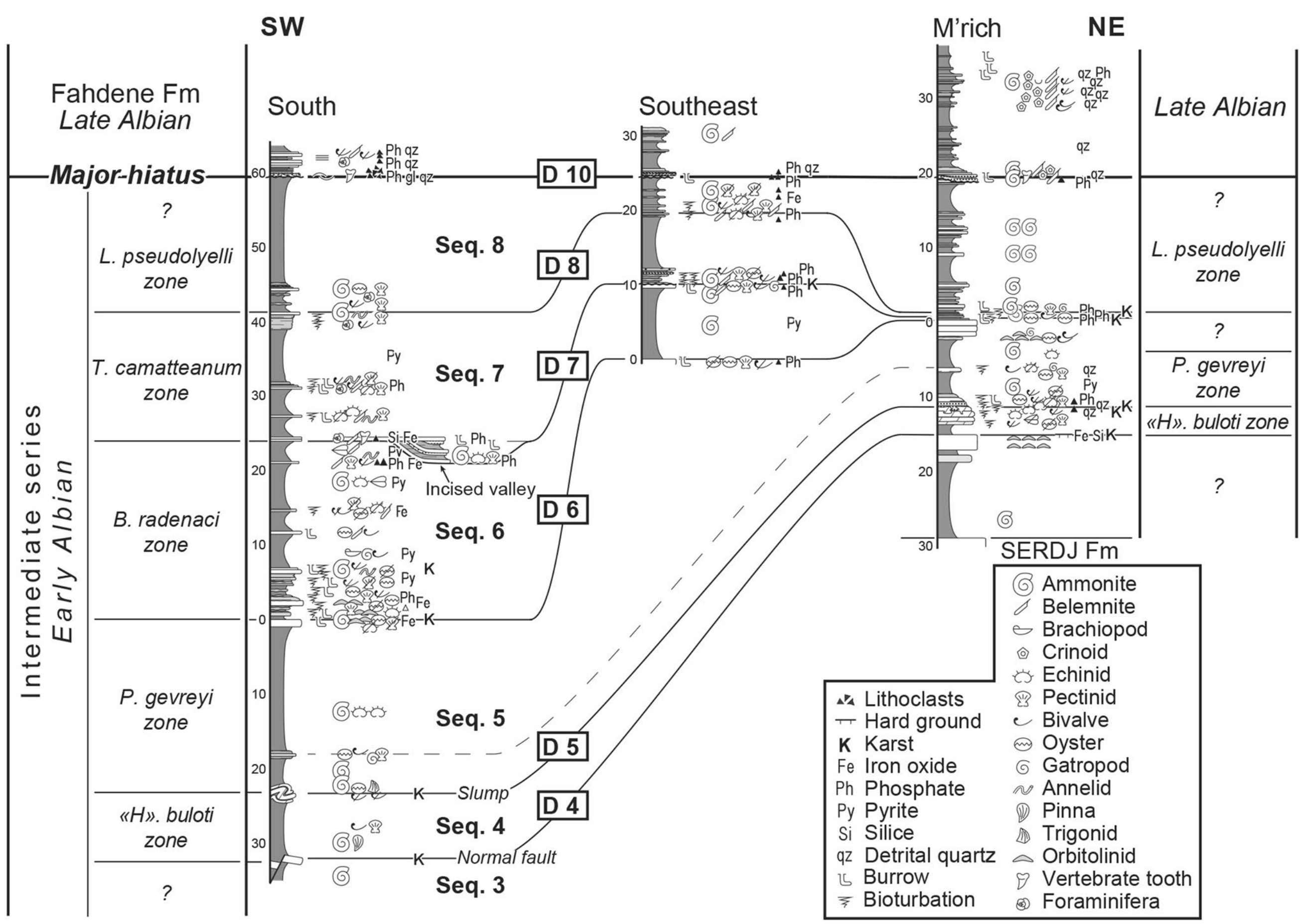

Fig. 6 Selected sections of the Intermediate series and Fahdene Formation of Jebel el Hamra: lithology, sedimentary features and correlations. Location on Fig. 3

southward tilting between deposition of S5 and S6 (Jaillard et al. 2013). At the base, a few calcareous beds contain abundant shallow-water benthic fauna (ostreids, pectinids and other bivalves, sea urchins, orbitolinids). They are overlain by marls with few beds of argillaceous limestone, yielding outer shelf benthic and pelagic fauna (sea urchins, pectinids, belemnites, ammonites). The top of S6 is marked to the Northeast by a massive, karstified limestone bed, and to the Southwest, by an erosional surface.

In the southern section, Sequence 7 begins with a lens-shaped, 2 m thick unit of phosphate-rich marlstone, sandy limestone and calcarenite. Since this unit yielded ammonites unknown in other sections and is restricted to a zone of the southern tip of jebel El Hamra, it is interpreted as the infilling of an incised valley. In this interpretation, the underlying sequence boundary D7 would be a major discontinuity, responsible for the emergence of the area. Sequence E is a marly succession with thin calcareous intercalations, the number of which increases toward the Northeast. It ends up with a bundle of calcareous beds containing a benthic fauna (pectinids, buchidae, annelids, benthic foraminifera) and locally phosphatized clasts.

Sequence 8 shows a highly variable thickness, probably due to subsequent erosions (see below). The transgressive part of the sequence is made of alternating marl and limestone with scarce benthic fauna (pectinids, annelids, with subordinate ostreids, echinids and benthic foraminifera), which are overlain by a monotonous marly succession, probably of deeper marine environment (Fig. 6). The fauna indicates an outer shelf to hemipelagic environment.

In all sections of Jebel El Hamra, Sequence 8 is overlain by a thin set of sandy to gravelly beds, with phosphate-rich interbeds bearing numerous fish teeth and scarce ammonites near the base, and abundant crinoids and belemnites in the upper part (Fig. 6). In the northwestern part of the jebel, this discontinuity is overlain by a phosphate-rich crust containing numerous belemnites, ammonites and gravels.

Correlations

Correlations in the Tajerouine area

The identification of discontinuities and sequences, together with accurate ammonite dating, allows to propose correlations of the sequences identified in the Tajerouine area (Fig. 7). Correlations show that the thickness of the earliest Albian series (Hameima Fm) slightly increases toward the Southeast (Fig. 4), whereas the thickness of the early Albian succession (Fahdene Fm) roughly increases toward the Northwest, i.e. toward the north Tunisian basin.

In the lower Fahdene Fm, the phosphate-rich calcarenites of the Slata section correlate with thick successions of alternating marl and limestone in the El Goussa and Hameima sections, especially at the base of S6 (Figs. 5 and 7). Conversely, such marly successions are absent in the Bou el Haneche section located to the Southeast (Fig. 7). This suggests that part of the limestone products generated on, or around, the positive swell of jebel Slata has been exported around the Slata area, and mostly toward the basin, as already proposed at a smaller scale within Jebel Slata (see Jaillard et al. 2013). In this interpretation, since the phosphate-rich calcarenite beds are located at the base of the S4 to S7 sequences, the calcareous successions observed at the base of the same sequences in the El Goussa and Hameima sections (Fig. 11c) can be interpreted as Lowstand deposits (Fig. 7). As a matter of fact, assuming that the margin was sloping on average toward the North or Northwest, the southeastern areas of the basin were topographically higher and locally emergent during low sea-level periods, and could not receive any of the carbonate exported at that time.

Following this assumption, the lack of phosphate-rich calcarenites before S4 and after S7 in jebel Slata, and the fact that the thicknesses of the Hameima Fm (Fig. 4) and Allam limestone in the Slata section (S7 and S8, Figs. 5 and 7) are comparable to those of other sections, suggest that the diapir located beneath jebel Slata was mainly active during deposition of S4 to S6. It is possible that the reduced thickness of S7 and S8 in the Jerissa section (Allam limestone) is due to a similar phenomenon; however, the lack of data on the Lower Shales in this section does not allow to conclude.

Correlations between the Tajerouine area and Jebel El Hamra

As evidenced by the biostratigraphic data, the first deposited early Albian sequences (S1, S2; Hameima Fm) are not represented in jebel El Hamra (Fig. 8). This means that in the latter area, the emergence period initiated by the drastic sea-level drop recorded at the Aptian-Albian boundary (Haq 2014) lasted longer than in the Tajerouine area. However, our observations do not advocate tectonic causes, since tectonic instabilities in these areas are mainly recorded from S3 onwards (Jaillard et al. 2013). Therefore, even though tectonic uplift cannot be ruled out, we propose that this hiatus was mainly of eustatic origin.

In general terms, the thickness of the intermediate series of Jebel El Hamra is much thinner than its time equivalent in the Tajerouine area (Fig. 8). This suggests that subsidence was much lower in the proximal Jebel El Hamra area, a classical feature of passive margins, in which the higher lithospheric stretching in distal areas induces a higher thermal subsidence (Allen and Allen 1993). However, the presence at the base of some sequences of incised valleys in Jebel el Hamra (D7, Figs. 6 and 8) indicates that this

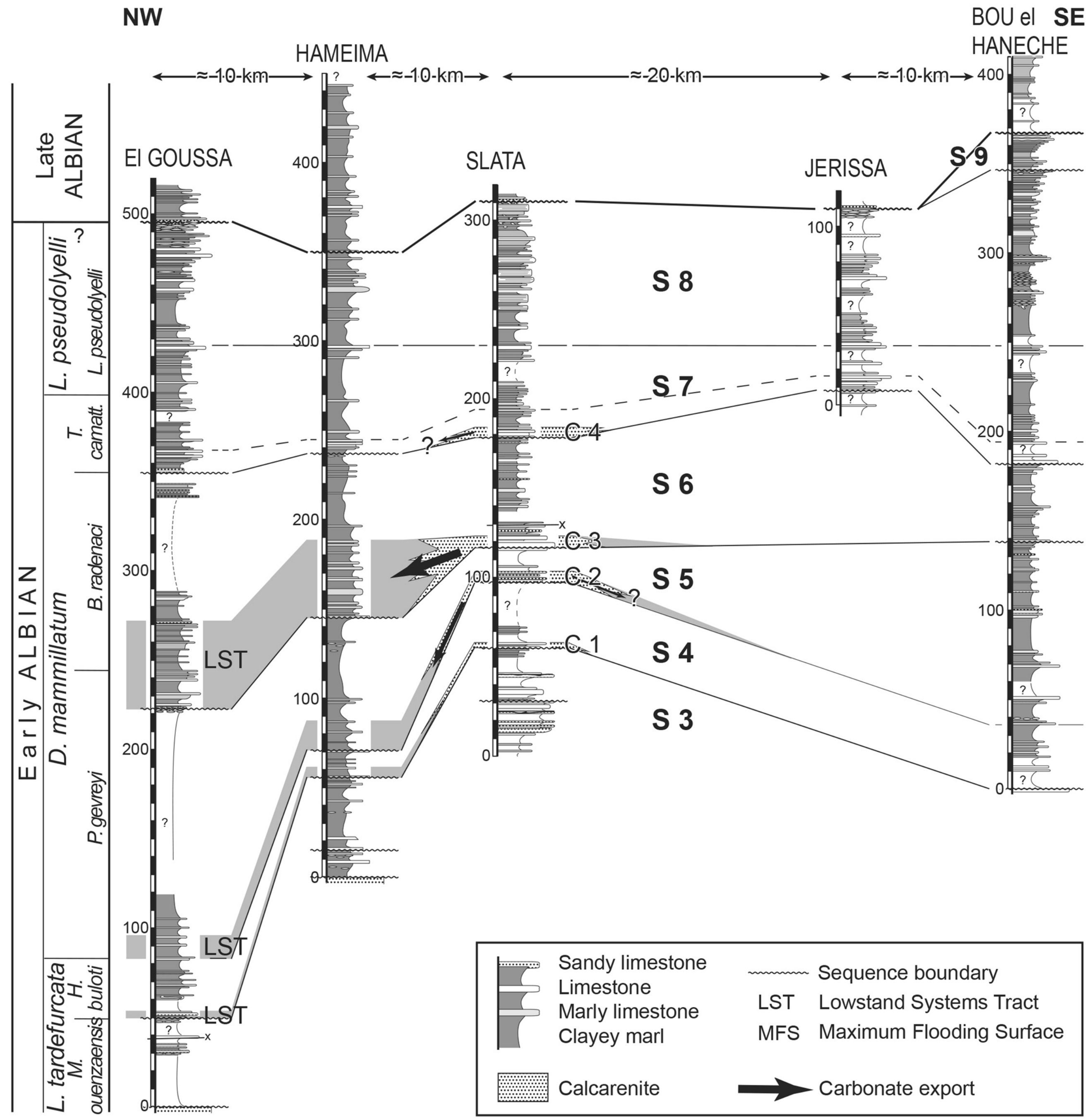

Fig. 7 Correlations of the sections studied in the Tajerouine area

area became frequently emergent during early Albian sea-level falls, and therefore, that marine transgression may have occurred later than in the distal Tajerouine region, thus accounting for part of the thickness reduction. Following this view, the intermediate series of Jebel El Hamra recorded sediments mainly deposited around the Maximum Flooding periods.

Relative importance of discontinuities

Among the identified sequence boundaries, most are marked by clear erosional surfaces (see above). However, although correlatable through most of the studied sections other discontinuities are only inferred from the presence of phosphate-rich layers, or from the end of a thickening-upward evolution (e.g. D5 and D8). Considering that erosional

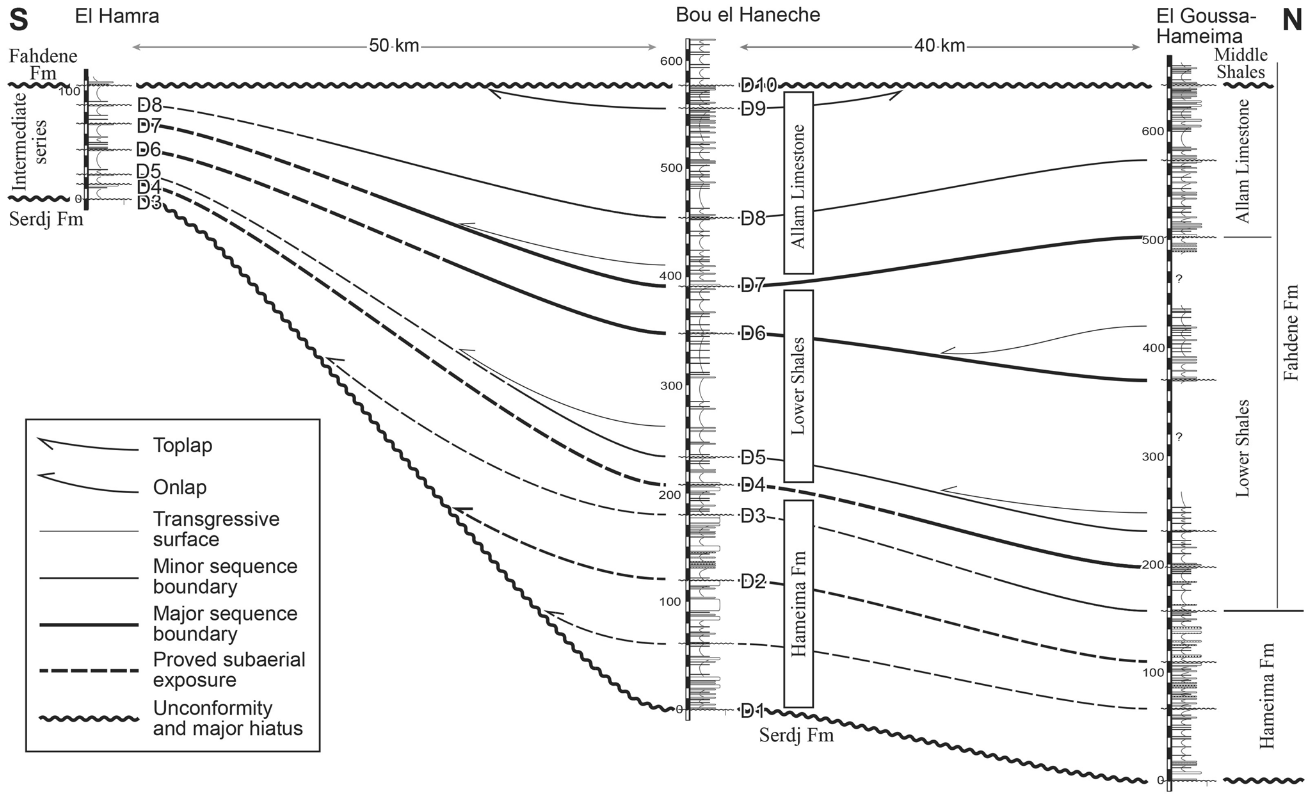

Fig. 8 Correlations between the Tajerouine and El Hamra areas

surfaces, widespread correlations, and significant facies changes are criteria for major sequence boundaries, the most important ones seem to be D1, D4, D6, D7 and D10 (Fig. 8).

D1 corresponds to an emergence period marked by widespread karsts, and thus to a stratigraphic hiatus due to subaerial exposure. It is dated as close to the Aptian-Albian boundary as defined by ammonites (Latil 2011), and roughly coincides with a major sea-level drop of latest Aptian age (KAp7 of Haq 2014). Many workers interpret this discontinuity as related to an extensional tectonic activity (e.g. Zouaghi et al. 2011; Ghanmi et al. 2017). However, we propose that in the study area, it was mainly controlled by eustacy (Jaillard et al. 2013; Ben Chaabane et al. 2019), although tectonic uplift may have locally played a role. Farther Southeast, however, the coeval sedimentary hiatus encompasses a much longer time span, and contains deformation of latest Aptian to middle Albian times (Jaillard et al. 2013), thus giving the impression of a single deformation occurring around the Aptian-Albian boundary (e.g. Lazzez et al. 2008; El Rabia et al. 2018).

Since the carbonate shelf sedimentation ended up at D4 in jebels Slata, Jerissa, Bou el Haneche and Ajered, i.e., over a distance of almost 50 km, S4 (base of *H. buloti* local zone, base of the *D. mammillatum* standard zone) represents a major backstepping stage, and thus, coincides with a major rise of relative sea level. This event followed an emergence period indicated by karsts in the southern areas, and suggested by the occurrence of shallow marine benthic fauna at the base of S4 in the Slata, Hameima and el Goussa sections (Figs. 5 and 7).

D6 is a karstified surface in jebel El Hamra (Fig. 6), and is marked in the Tajerouine area by a conspicuous and constant limestone bed containing phosphatized lithoclasts (Fig. 5). Locally, the presence of oyster fragments (Hameima, Fig. 5) suggests a shallow marine deposition for this basal bed. Thus, although no clear evidences of subaerial erosion have been observed, local emergence of the Tajerouine area cannot be ruled out.

In Jebel El Hamra, D7 is marked by an incised valley (Fig. 6), indicating an emergence period and a significant sea-level drop. In the Tajerouine area, beds overlying D7 are virtually devoid of benthic fauna, and are locally made of phosphate-rich calcarenites (Fig. 5), suggesting a period submarine erosion or condensation. Discontinuity D8 does not comprise a phosphate-rich bed in jebel Slata, nor an erosional surface in other sections (Figs. 5 and 6), the average depositional depth of S7 and S8 seems to be greater than that of earlier sequences. Therefore, deposition of S7 (base of the *T. camatteanum* local zone, top of the *D. mammillatum* standard zone) is interpreted as related to a significant sea-level rise that followed a significant sea-level drop (D7).

The major unconformity D10 corresponds to a hiatus of the whole middle Albian substage (Chihaoui et al. 2010; Latil 2011; Jaillard et al. 2013). In the overlying transgressive lag, scarce ammonites indicate both a middle (*L. Lyelli*) and late Albian age (*Mortoniceras* (*Deiradoceras*) sp., *Venezoliceras* sp., *Mirapelia* sp.) (Latil 2011). This indicates that (1) deposits of middle Albian age are absent, this stage being mainly represented by a sedimentary hiatus (Chihaoui et al. 2010; Latil 2011), (2) marine sedimentation occurred temporarily, however, at least during earliest middle Albian times (*L. Lyelli* ammonite zone), (3) this discontinuity is a major sedimentary event (Jaillard et al. 2013), as shown by local smooth angular unconformity (M'rich area), and (4) a new marine transgression occurred in jebel El Hamra in early (not earliest) late Albian times (Latil 2011). In northwestern Algeria, Masse and Thieuloy (1979) also mentioned *L. lyelli* in the transgressive bed overlying the discontinuity, which indicates that emersion occurred in middle-to-late-middle Albian times. This unconformity, thus, likely corresponds to that mentioned at 109.3 Ma by Haq (2014).

Interpretations and discussion

Origin of the Hameima Sandstones

Intercalations of sandstone beds in carbonate shelf deposits can be classically interpreted as the progradation of continental or shoreline clastic deposits onto very shallow marine carbonates (e.g. Emery and Myers 1996), or as reworked material deposited after an erosion period (transgressive lag, e.g. Hwang and Heller 2002; Cattaneo and Steel 2003). In the Hameima Fm, sandstone of S2 contains shallow-to-open marine fauna (algae, urchins, bivalves, belemnites, ammonites), so that the first interpretation can be ruled out. One may also propose that a relative sea-level fall may have enhanced deposition of a shallow marine, clastic body onto deeper marine sediments, therefore representing a LST (e.g. Emery and Myers 1996). However, on the one hand, sand beds are known both in the lower (retrograding, deepening upward), or upper (prograding, shallowing upward) parts of S1 and S3 (Fig. 4), and are thus not dependent on sea-level variations or on shoreline migration. On the other hand, the marine fauna contained in the Hameima sandstones is not significantly shallower than that of the underlying strata, as should be the case for a LST. Moreover, except very local and sporadic clastic systems (Nasri et al. 2017), no coeval significant fluvial system of early Albian age is known farther South and Southeast in the Kebar Fm (Trabelsi et al. 2010; 2015; Salmouna et al. 2017; Houla et al. 2017) or in the Chott area (Ben Youssef and Peybernès 1986; Abdallah et al. 1995; Hfaied et al. 2013), and the karstic cavities in Jebel El Hamra or in Jebel Semmama (Touir et al. 2015) are not filled by quartz-rich deposits. Thus, the emergent area was probably not marked by important fluvial systems able to feed the Hameima sandstones. Finally, the Hameima sandstones are fine-grained, clean and very well sorted, and do not contain gravels or lithoclasts, if one except local eolian quartz. Thus, the interpretation of the Hameima sandstones as the basal lag of a marine transgression is unlikely.

Dubourdieu (1956) noticed that the size of the quartz grain decreased toward the Northeast and through time. This was then confirmed by Vila (1980) and Fabre (2005), who showed that the source of the early Albian sands was the Saharan shield located in southern Algeria, and by Masse and Thieuloy (1979), who proposed that the early Albian sands of northeastern Algeria proceeded form the Southwest. Following these authors, we propose that the Hameima sands were fed by a clastic system located in present-day southern Algeria, Southwest of Tunisia. The distribution of these sands in northern central Tunisia may be due either to Eastward currents acting on the Algerian shelf (Vila 1980), or to a rejuvenation of the Saharan shield related to the rifting of the Atlantic Ocean at Equatorial latitudes during the early Albian (Moulin et al. 2010).

Studying a comparable quartz-rich interval in the Aptian carbonate shelf (Serdj Fm), Heldt et al. (2010) also proposed that it resulted from increased coastal runoff. These authors interpret the recovery of the carbonate sedimentation after this mid-Aptian clastic crisis as the result of an arid climate that limited the nutrient input proceeding from the Saharan hinterland (Heldt et al. 2010). A comparable interpretation may be proposed for the Hameima Fm, since S3 is still locally dominated by carbonate shelf deposits (Jerissa, Bou el Haneche, Fig. 4). On the other hand, a distal, aeolian origin of these fine, well-sorted quartz grains cannot be ruled out, but their subsequent reworking by marine processes makes difficult to document this hypothesis.

Nature and origin of the sedimentary discontinuities

In the Albian series of Central Tunisia, sequence boundaries are marked by (1) karstic features observed at the top of limestone beds, or by erosional surfaces overlain either by (2) sandy accumulations or concentrations of ammonites and bioclasts, or (3) calcareous beds containing calcareous clasts, the rim of which is phosphatized or mineralized, or (4) phosphate-rich calcarenites (Figs. 9, 10, 11).

Karstic surfaces

In the Hameima Fm (Tajerouine area), sedimentary discontinuities are usually marked by karstic surfaces observed

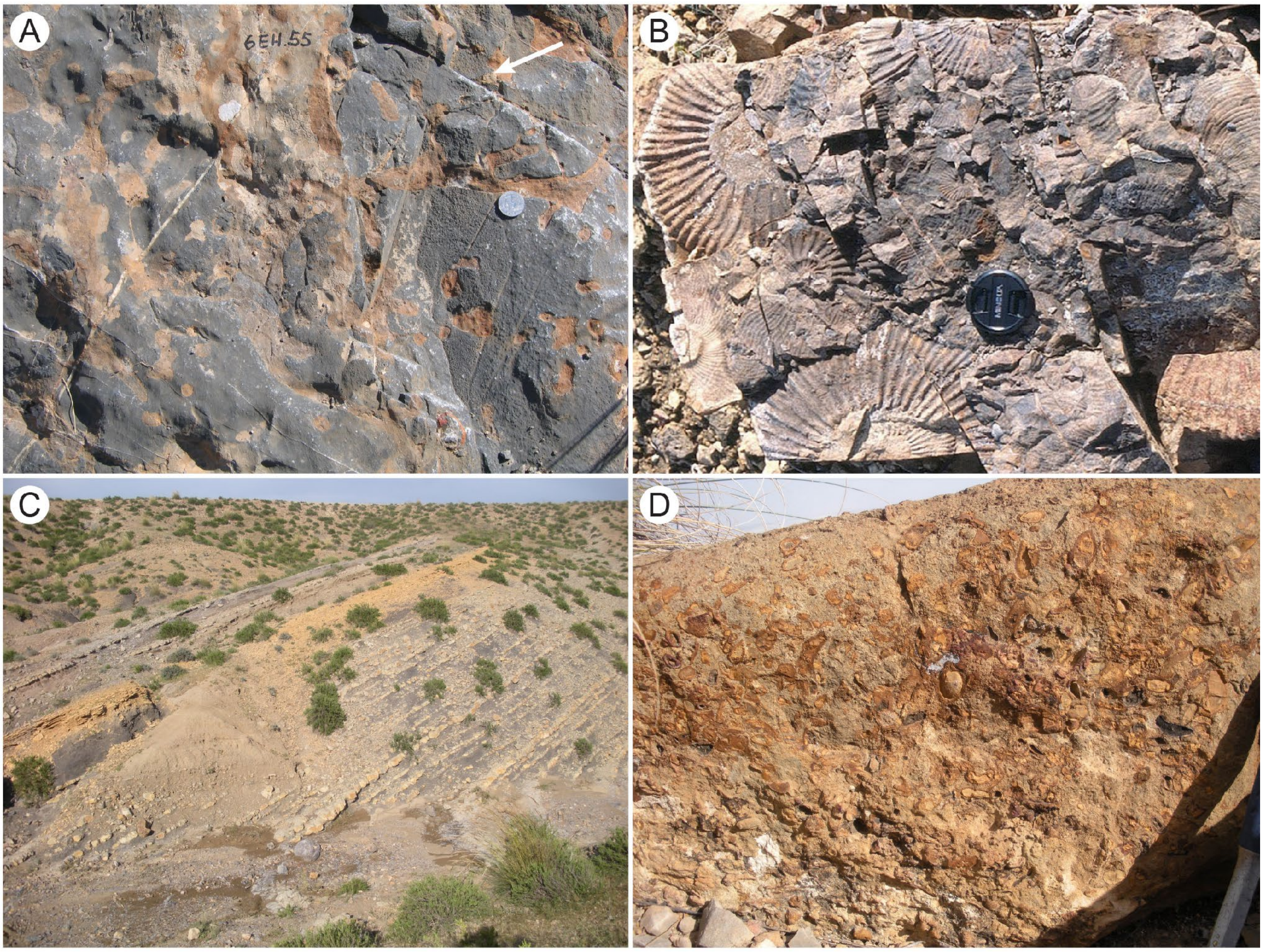

Fig. 9 Photographs of some sedimentary discontinuities observed in the Early Albian succession. **a** Karstic surface: Hameima Fm, Jebel Bou el Haneche section, m. 118. **b** Accumulation of ammonites: Fahdene Fm, Hameima section, m. 103. **c** Thick yellow sand bed: Fahdene Fm, Jebel Slata section, m. 446. **d** Matrix-supported conglomerate, with rounded calcareous clasts coated by iron oxides: Fahdene Fm, base of the Upper Albian series, Eastern flank of Jebel Slata

on top of calcareous beds (Fig. 9a). The same features are observed in the lower part of the Intermediate Series of jebel El Hamra. They undoubtedly mean subaerial exposure and dissolution by meteoric waters. In the Slata section, the karstified surfaces are locally incised by fossil river channels (Chihaoui 2009) (m 160, Fig. 4).

Concentrations of ammonites

Accumulations of ammonites can be observed either at the base of calcareous beds overlying erosional surfaces (Fig. 9b), or within a muddy marl succession. In both cases, concentration of ammonites suggests that during erosion, the fine-grained part of the formerly deposited sediments was removed, exhuming already lithified fossils that rested on the erosional surface.

In the first case, ammonites are observed associated with abundant benthic fauna (mainly bivalves). This, together with the calcareous nature of the enclosing bed suggests a shallow marine environment during the transgression that follows the discontinuity. Thus, the sedimentary discontinuity may be due to exposure and subaerial erosion.

In the second case (D7 in Hameima, D6 in El Goussa), the ammonites locally proceed from significantly older strata, supporting the interpretation of a deep erosion of the fine-grained sediments. Since neither emergence evidences, nor limestones bed, nor associated benthic fauna are observed, erosion is likely to have been submarine.

Sand beds

In the lower Fahdene Fm, sedimentary discontinuities may be overlain by fine-grained sand accumulations forming

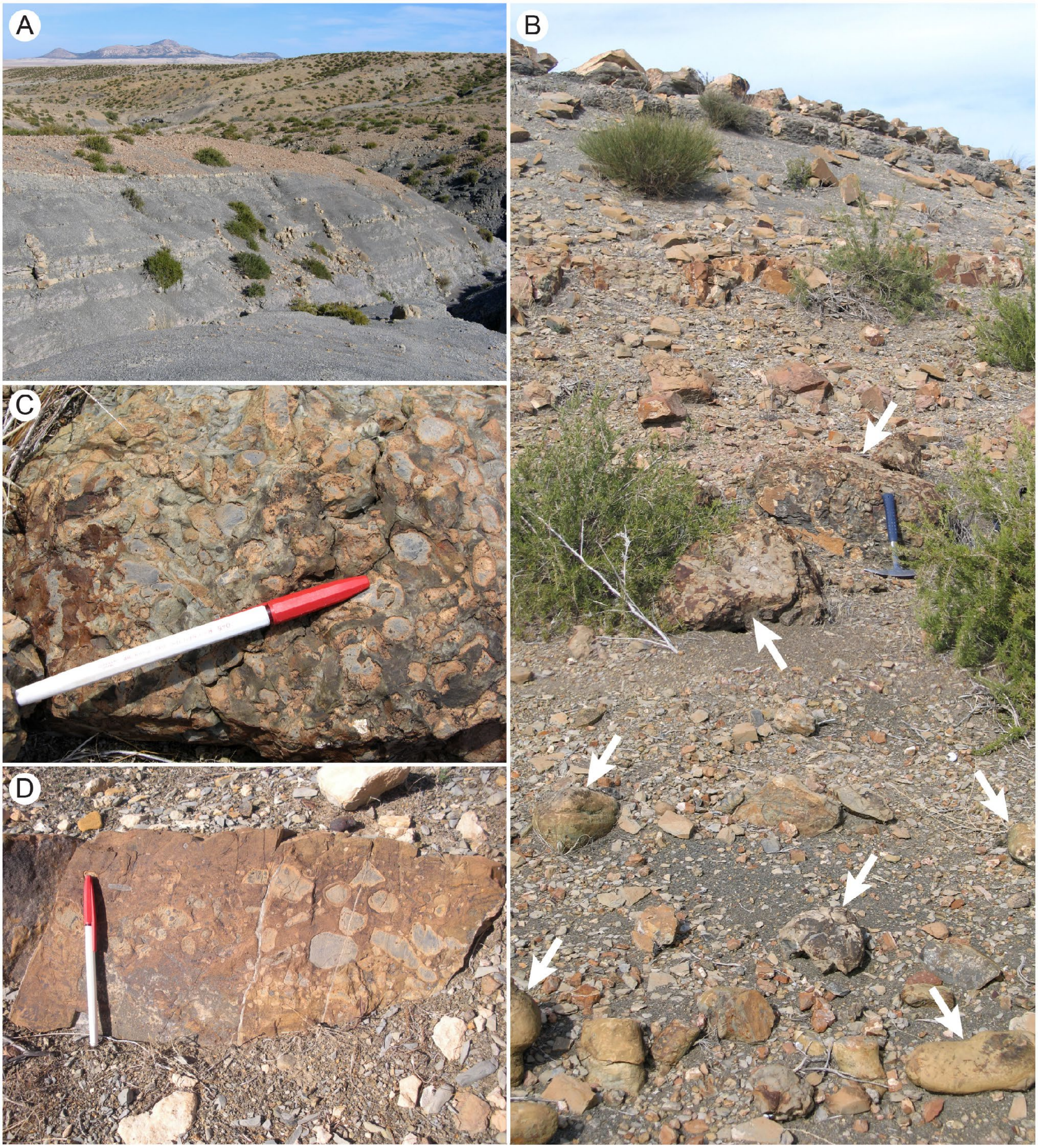

Fig. 10 Photographs illustrating the formation of phosphate-rich calcareous clasts in the Fahdene Fm. **a** Vertical calcareous concretions, Jebel Slata section, m. 435–450. Note the overlying reddish sandstone underlining the Late Albian transgression. **b** Loose and in situ septarian calcareous concretions (white arrows), El Goussa section, m. 215–232. **c** Partially fragmented septarian calcareous concretion, El Goussa section, m. 223. Note the phosphatized rim of the fragments. **d** Matrix-supported calcareous conglomerate with reworked phosphatized clasts, Hameima section, m. 194

either thin, lens-shaped, poorly marked sand layers, or rarely, by thicker continuous beds (middle Albian major discontinuity D10, Figs. 9c, 10a). In the first, most frequent case, no sedimentary features are observed, and the presence of ammonites below and within the sand bed suggests a submarine erosion period. In some cases, the sandy lenses contain oil (Hameima, Jerissa and El Goussa sections). In the second case, poorly preserved laminations and current ripples are observed. In both cases, the concentration of fine-grained sandstone on the erosional surface is interpreted as the product of the removal of the fine-grained, clayey fraction of the underlying sediments during erosion. However, in the case of a thin, lenticular sand layer, erosion may have been submarine (Hameima, Jerissa, Bou el Haneche, El Goussa), whereas the shallow marine sedimentary features observed in thick, transgressive sand beds (D10 in Slata section) suggest that they may seal a subaerial erosion surface.

Conglomerates or breccias

Three kinds of conglomerate or breccia have been observed. The first one is a matrix supported breccia containing various calcareous clasts, mainly angular, of distinct origin. It has only been observed in the northwestern part of Jebel Slata. The second type of conglomerate contains rounded calcareous clasts, coated by iron oxides (Fig. 9d). These two types of conglomerates overly the major, middle Albian discontinuity (D10), and have been mainly observed in jebel Slata and jebel El Hamra. They are, therefore, interpreted as the result of the subaerial erosion occurring in the middle Albian, then reworked during the late Albian marine transgression.

The third type of conglomerate presents subangular to subrounded clasts of micritic limestone, presenting phosphatized rims (Fig. 10d) and has been observed in various sections. Observations on these sections make possible to interpret their formation process. Septarian calcareous concretions have been observed below several major discontinuities (D7 in Hameima, D9 in Bou el Haneche, Fig. 4; D6 in El Goussa) (Fig. 10a, b). In some cases the calcareous concretions show a vertical arrangement (Fig. 10a). Note that similar vertical concretions have been observed in the Tajerouine area, below the discontinuity of the Albian-Cenomanian boundary (Fig. 12 of Robaszynski et al. 1993). Such septarian concretions are thought to form during early diagenesis by biocarbonate precipitation through sulphate reduction during periods of reduced sedimentation or hiatuses (Raiswell and Fisher 2004; Hendry et al. 2006; Alessandretti et al. 2015). In the El Goussa section, the discontinuity is marked by an accumulation of micritic calcareous fragments, regarded as the calcareous part of the septarian concretions, cemented by mineralized, oxide- and phosphate-rich matrix (Fig. 10c). The micritic calcareous fragments exhibit phosphatized rims and are quite similar to those found in the third-type conglomerate (Fig. 10d). Therefore, we propose that the following scenario occurred during the hiatus associated to this kind of discontinuity: (1) septarian calcareous concretions formed a few meters below sea-floor through sulphate reduction, (2) erosion of the soft sediment exhumed the septarian concretions, (3) erosion and dissolution isolated the calcareous micritic parts of the septarian concretions, (4) these micritic elements accumulated on sea-floor and there rim was progressively mineralized and/or phosphatized, and (5) they were either cemented in situ (Fig. 10c), or more commonly, reworked in the subsequent transgressive calcareous deposits (Fig. 10d). In this interpretation, erosion can be either subaerial, or submarine, but mineralization likely occurred in a submarine environment, probably favored by circulation of mineralized waters, likely through upwelling currents.

Phosphate-rich calcarenite

Phosphate-rich calcarenites are only known in the Slata section (C1 to C4, Fig. 5) and overly discontinuities D4 to D7 (Fig. 5). It consists of coarse-grained, poorly sorted calcarenite with a soft, white-to-yellow, phosphate-rich marly matrix. It contains rounded litho- and bio-clasts among which brachiopods, sea urchins, bivalves, orbitolinids and belemnites (Fig. 11a). Bioturbation is locally common (Fig. 11b). The surface of the lithoclasts is frequently oxidized and mineralized. The coarse-grained and rounded nature of the clasts indicate deposition in a high-energy regime. The abundance of phosphate suggests a condensed sedimentation and the occurrence of upwellings (Parrish and Curtis 1982; Föllmi 1996; Pufahl and Groat 2017). Condensed sedimentation is supported by the reduced thickness of the Slata section during the early Albian (S4 to S6, Fig. 5). Therefore, these beds are interpreted as deposited on a swell submitted to currents or storm waves. According to Jaillard et al. (2013), this positive high would be generated by the growth of a diapir located below the present-day jebel Slata (see also Smati 1986; Rddad et al. 2019).

Characters of the early Albian sedimentation

No high-energy facies were observed in the early Albian deposits of the studied area, except in some layers of the Slata section. Low-angle cross-bedding and current ripples were observed at the base of the Hameima sandstones

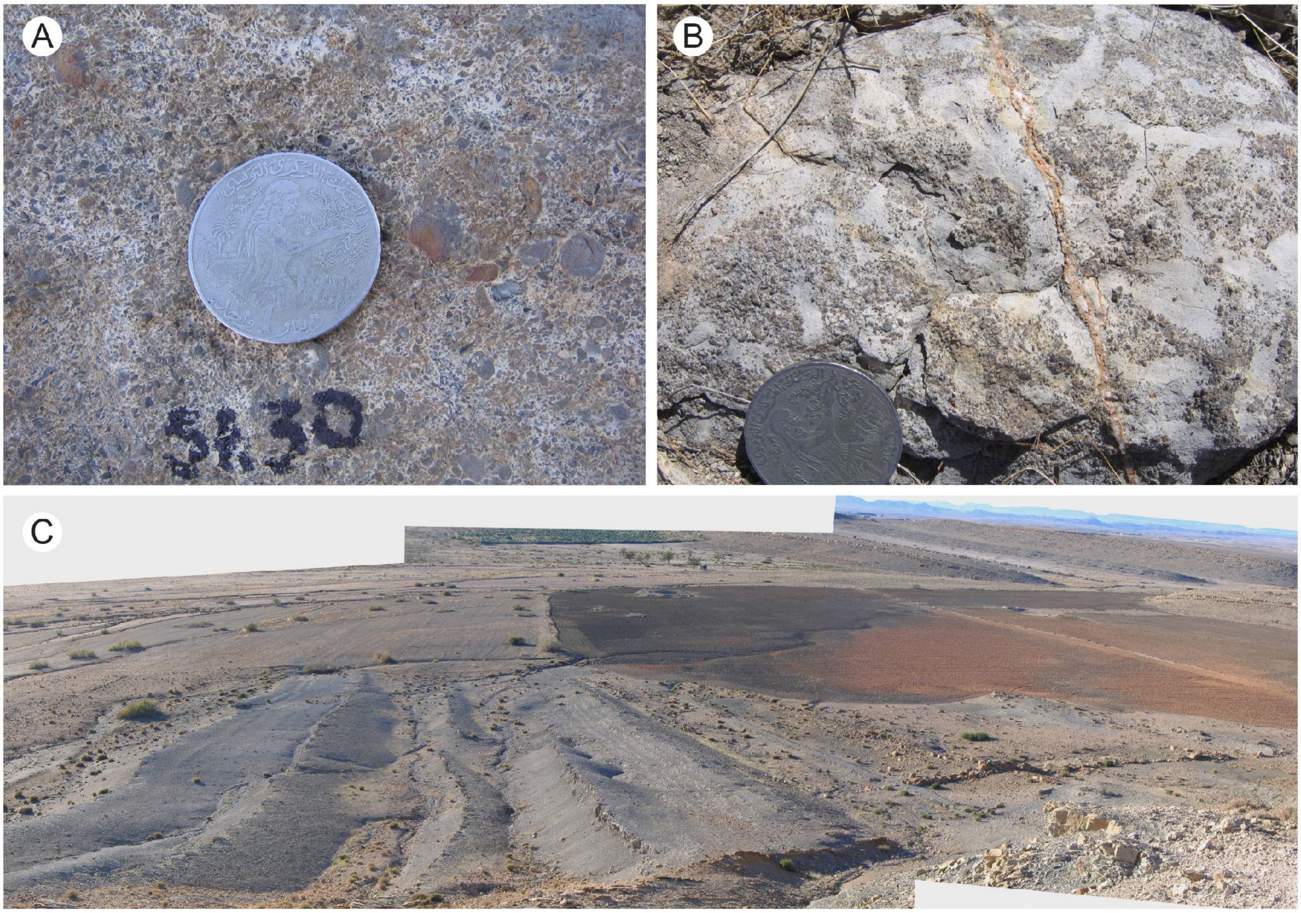

Fig. 11 Field photographs of the Fahdene Formation. **a** Phosphate-rich, poorly sorted calcarenite. Slata section, m. 257 (C3 on Fig. 5). **b** Bioturbated phosphate-rich calcarenite, Slata section, m. 314 (C4 on Fig. 5). **c** Marly base of S5, Hameima section, m. 190–250 (top to the right)

(S2b), as well as local Hummocky Cross Stratification in some sandstone beds of S1 and S3 (Fig. 5). In carbonates, neither oolites, nor corals or current features were observed, indicating an overall low-energy regime of deposition. This leads to interpret the Albian Tunisian margin as a low-energy, low-dipping ramp (Tucker and Wright 1990).

Such a low-energy regime can be related to the paleogeographic location of the Tunisian margin on the south Tethyan margin. The Tethys was an ESE–WNW trending ocean located in the northern hemisphere, and its southern shore was located at 10°N to 20°N and submitted to westward blowing Trade Winds (Trabucho-Alexandre et al. 2011). Because of the Coriolis force, winds and storms generated in the ocean were deflected to the North (right), i.e. to the northern shore of the Tethys Ocean, where varied and commonly high-energy facies are observed (e.g. Arnaud-Vanneau and Arnaud 1990; Tesovic et al. 2011; Basilone and Sulli 2018; Tendil et al. 2018). As a result, on the one hand, the Tethys Ocean was the site of a clockwise oceanic gyre, as modelled by Pohl et al. (2019) for Aptian times (Fig. 12), and on the other hand, the southern shore of the Tethys was sheltered from tropical storms, thus explaining its average low-energy regime. Moreover, the excess of surface water drifted northward by the Coriolis force had to be balanced by the upwelling of deep water (Ben Fadhel et al. 2011, 2014), as observed presently on the western shores of North–South trending oceans. The flow of such deep, cold and mineralized deep water may account for the phosphatization of calcareous clasts (Fig. 12) during submarine hiatuses (see above).

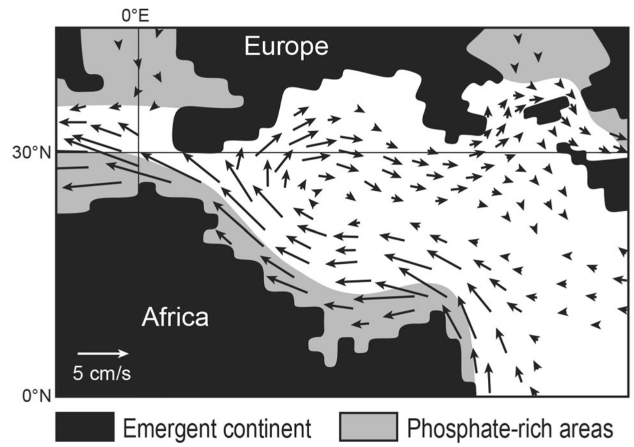

Fig. 12 Oceanic circulation in the Western Tethys, from Pohl et al. (2019), simplified

As mentioned above, the only noticeable high-energy facies were observed in the Slata section, at the base of S4 to S7 (calcarenites C1 to C4, Fig. 5), suggesting that this site acted as a swell, related to halokinetic movements (Jaillard et al. 2017). If so, this means that the surficial part of the water column was the site of significant energy, likely related to tides or waves. This agitated surficial water column can explain the submarine erosion of sea floor during low sea-level periods (wave ravinement surface, Cattaneo and Steel 2003), as observed in D5 to D7 in the Tajerouine area (Fig. 5).

Phosphate formation and stratification of the water column

Precipitation of phosphatic minerals occurs in the sediment, close to the sediment–water interface, thanks to microbial mediation, in suboxic conditions and is mainly favoured by the proximity of upwelling currents (Parrish and Curtis 1982; Lamboy 1990; Briggs et al. 1993; Föllmi 1996; 2016; Mort et al. 2008; Salama et al. 2015; Puhfal and Groat 2017). As a matter of fact, phosphorus-rich water brought by upwellings favors high organic productivity. The organic activity and degradation of the resulting organic matter in turn consume dissolved oxygen, and induce the formation of a zone of dysoxic water culminating in the oxygen-minimum zone located in the distal part of the shelf, explaining the frequent association in the geological record of phosphorus and organic-rich sediments (e.g. Parrish and Curtis 1982; Föllmi 1996; Puhfal and Groat 2017), as also observed in Albian deposits of eastern Algeria (Bentaalla-Kaced et al. 2017). Phosphate-rich deposits may result, either from sediment starvation, or more frequently, from sediment starvation, erosion, reworking and winnowing (Föllmi 1996; 2016). Therefore, they are more frequent in transgressive deposits (Föllmi 2016; Baioumy et al. 2005; Compton and Bergh 2016; Puhfal and Groat 2017).

In the study area, phosphatized clasts are found in conglomerates overlying sequence boundaries in outer ramp settings, while phosphate-rich deposits occur in the sandy infill of incised valley (El Hamra), as shallow marine marls (El Hamra), or as the matrix of calcarenites on isolated swells (Slata), always near the base of third-order sequences (Figs. 5 and 6). They, thus, correspond to transgressive deposits. In Jebel Slata (S5 to S7) and Jebel El Hamra (S5 to S8), after erosion and accumulation of calcarenite by the oxic, agitated surficial water during low sea level, phosphate was probably formed during transgressive intervals. During the latter periods, high-frequency sea-level fluctuations provoked the alternation on the sea floor of oxic water favorable to bioturbation and condensation, and of suboxic water that allowed phosphate formation and concentration. The location of phosphate-rich sediments in incised valley in Jebel El Hamra suggests that they may have been reworked and transported landward from the middle ramp, as proposed by Salama et al. (2015) for part of the Late Cretaceous phosphorites of Egypt. Then, as sea level rose, the oxic/suboxic waters interface was no longer in contact with sea floor, phosphate-rich marls deposited, which were followed by dark clayey marl as phosphate generation ceased.

Therefore, the presence of these phosphate-rich deposits suggests that the water column of the Tunisian margin comprised a suboxic zone favorable to phosphate precipitation, which separated oxic, agitated upper waters, responsible for erosion, winnowing and concentration of phosphate during low sea-level periods, and dysoxic, low-energy waters, responsible for the deposition of dark, little bioturbated and little fossiliferous marls. Considering the low-energy nature of the early Albian sedimentation in Tunisia, the surficial, oxic, agitated water layer might have been thin, may be 10 m thick. The phosphate-rich matrix of calcarenites, and the occurrence of phosphate-rich matrix in incised valley fills suggests that the suboxic water strata was located immediately below the surficial oxic water layer. Since phosphate-rich deposits are relatively thin (<15 m), the dysaerobic water strata might have appeared at relatively shallow depth, probably no more than a few tens of meters. The presence of relatively shallow O_2-depleted water, adverse to carbonate production, may partly account for the scarcity of carbonate deposits in the upper part of the early Albian series of Central Tunisia.

According to this model, at the beginning of the early Albian transgression (S1 to S3, Fig. 13), Jebel El Hamra remained emergent most of the time, and deposition in the Tajerouine area occurred within the upper oxic part of the

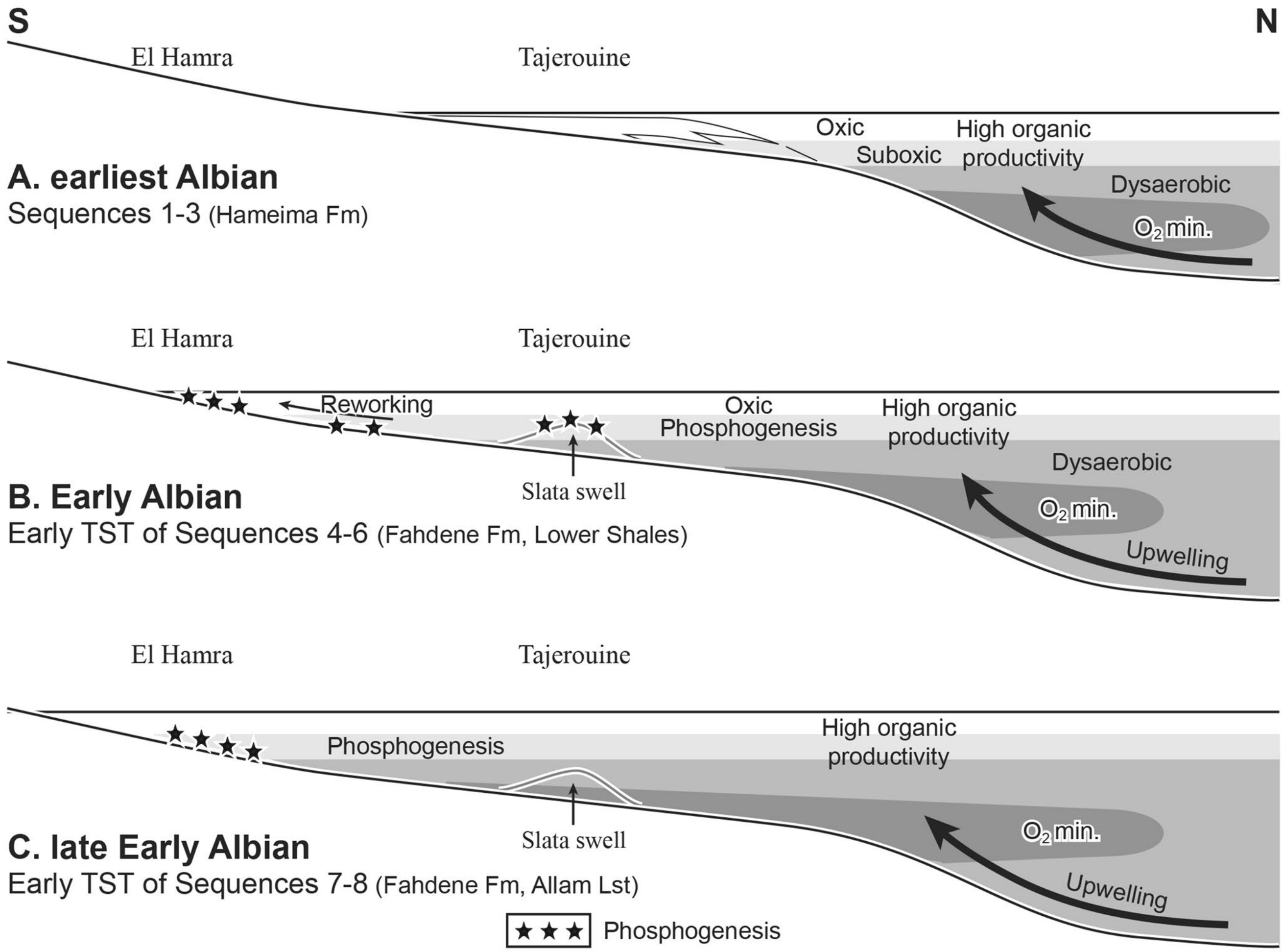

Fig. 13 Model for the evolution of the Tunisian margin during the Early Albian transgression, explaining the genesis of phosphate-rich and organic-rich deposits

water column, allowing deposition of dominantly calcareous shelf sediments (Hameima Fm, Fig. 13).

Later (S4 to S6, Fig. 13), the marine transgression reached the El Hamra area, causing the concentration of phosphate during the early phases of transgressions. Meanwhile, the Tajerouine area was mostly located in the O_2-depleted, lower part of the water column, explaining the deposition of dark argillaceous marls with scarce benthic fauna (Lower Shales). Because it was uplifted by the incipient halokinetic activity, the Slata area was located in the suboxic water strata, during low sea-level periods, favoring phosphate precipitation.

As deposition depth increased during the early Albian eustatic rise (Haq 2014), the Tajerouine area remained below the suboxic water strata, and the O_2 minimum zone encroached onto the Tunisian margin (Khalifa et al. 2018), giving way to the deposition of the dysoxic, laminated, no bioturbated carbonates of the Allam Limestone (S7 to S9) (Fig. 13). Meanwhile, the shallower area of Jebel El Hamra remained submitted to the fluctuating suboxic zone, as supported by the phosphatic beds at the base (early TST) of S5 to S8 and the lack of black-laminated limestone beds (Fig. 6).

Conclusion

The detailed study of various sections of the Lower Albian series of Tajerouine and Thala areas and of their ammonite fauna allowed to distinguish several 3rd order depositional sequences that can be correlated regionally. In the southern area (Jebel el Hamra), most sequence boundaries correspond to emergence periods, whereas in the northern Tajerouine area, sequence boundaries are materialized by karstified surfaces in the lower sequences, and by submarine erosional surfaces in the upper sequences. Submarine erosion of outer shelf marls likely resulted from wave and tide energy agitating the surficial water, thus traducing low sea-level periods.

This, associated with upwelling currents were responsible for the phosphatization of lithoclasts, once exhumed by erosion and winnowing.

The organization of depositional sequences highlights the modalities of the early Albian marine transgression. The earliest sequences (*L. tardefurcata* ammonite standard zone) are represented by deposits of a mixed, carbonate/clastic shelf that are only recorded in the distal Tajerouine area. Two new transgressive pulses are recorded in the upper part of the *L. tardefurcata* standard zone, and resulted in the first Albian marine deposits in jebel el Hamra (*M. ouenzaensis* local zone), and in the complete drowning of the carbonate shelf in the Tajerouine area (*H. buloti* local zone). A third step in the early Albian transgression is marked in the *D. mammillatum* standard zone, by the diversification of the open marine fauna in jebel el Hamra (*B. radenaci* local zone) and by the development of dysaerobic conditions in the Tajerouine area. A last transgressive pulse near the top of the *D. mammillatum* zone (*T. camatteanum* local zone) is marked by a relative homogenization of the marine environments in the whole studied area and by dysaerobic conditions to the North. The early Albian transgression is then interrupted by the emersion, in the middle Albian, of large parts of the studied area. The resulting hiatus encompasses a large part of the middle Albian, and is followed by a stepped, late Albian marine transgression.

In the whole area, the overall energy of deposition is low, probably due to the location of the Tunisian margin on the southern shore of Tethys. The latter was, thus, sheltered from tropical storms that were deflected to the North by the Coriolis forces. The latter are also responsible for the formation of a clockwise oceanic gyre in this part of the Tethys, which favored upwelling currents on the Tunisian margin. In the Tajerouine area, however, high-energy deposits are locally and sporadically recorded, probably because of early diapir growth that created swells exposed to the agitated surficial waters. These local shoals were favorable to carbonate sedimentation, but most of these products were exported toward the distal parts of the margin. The occurrence of upwellings induced a stratification of the water column that comprised agitated, oxic surficial waters, suboxic intermediate waters in which phosphate could precipitate, and O_2-depleted deep waters. As sea level rose during the early Albian transgression, the O_2 minimum zone reached the Tunisian margin, explaining deposition of laminated, organic-rich sediments in the late early Albian (Allam limestones).

Acknowledgements We are grateful to the French-Tunisian scientific collaboration agreement PHC Utique n° 07G1008 funded by the Tunisian and French governments. The French Institut de Recherche pour le Développement (IRD) and the ISTerre Laboratory (Grenoble, France) supported this work. We thank H. Arnaud, F. Robaszynski and M. Bachman for fruitful discussions. Thanks are also due to S. Ferry and an anonymous reviewer, for their constructive suggestions.

References

Abdallah H, Memmi L, Damotte R, Rat P, Magniez-Janin F (1995) Le Crétacé de la chaîne nord des Chotts (Tunisie du centre-sud): stratigraphie et comparaison avec les régions voisines. Cretac Res 16:487–538

Alessandretti L, Veríssimo Warren L, Machado R, Felipe Novello V, Jamil Sayeg I (2015) Septarian carbonate concretions in the Permian Rio do Rasto Formation: birth, growth and implications for the early diagenetic history of southwestern Gondwana succession. Sediment Geol 326:1–15

Allen PA, Allen JR (2013) Basin analysis: principles and application to petroleum play assessment. Blackwell Publisher, p 265

Arfaoui M, Inoubli MH, Tlig S, Alouani R (2011) Gravity analysis of salt structures. an example from the El Kef-Ouargha region (northern Tunisia). Geophy Prospect 59:576–591

Arnaud-Vanneau A, Arnaud H (1990) Hauterivian to Lower Albian carbonate shelf sedimentation and sequence stratigraphy in the Jura and northern subalpine chains (southeastern France and Swiss Jura). Internat. Assoc. Sediment Spec Publ 9:203–233

Bahrouni N, Houla Y, Soussi M, Boughdiri M, Ben Ali W, Nasri A, Bouaziz S (2015) Discovery of Jurassic ammonite-bearing series in Jebel Bou Hedma (South-Central Tunisian Atlas): Implications for stratigraphic correlations and paleogeographic reconstruction. J Afr Earth Sci 113:101–113

Baioumy H, Tada R (2005) Origin of Late Cretaceous phosphorites in Egypt. Cretac Res 26:261–275

Basilone L, Sulli A (2018) Basin analysis in the Southern Tethyan margin: facies sequences, stratal pattern and subsidence history highlight extension-to-inversion processes in the Cretaceous Panormide carbonate platform (NW Sicily). Sediment Geol 363:235–251

Ben Chaabane N, Khemiri F, Soussi M, Latil J-L, Robert E, Belhajtaher I (2019) Aptian-lower albian serdj carbonate platform of the Tunisian atlas: development, demise and petroleum implication. Marine Petroleum Geol 101:566–591

Ben Fadhel M, Zouaghi T, Amri A, Ben Youssef M (2014) Radiolarian and planktic foraminifera biostratigraphy of the early albian organic-rich beds of fahdene formation, Northern Tunisia. J Earth Sci 25:45–63

Ben Fahdel M, Layeb M, Hedfi A, Ben Youssef M (2011) Albian oceanic anoxic events in northern Tunisia: biostratigraphic and geochemical insights. Cretac Res 32:685–699

Ben Youssef M, Peybernès B (1986) Données micropaléontologiques et biostratigraphiques nouvelles sur le Crétacé inférieur marin du Sud-Tunisien. J Afr Earth Sci 5:217–231

Bentaalla-Kaced S, Aïfa T, Deramchi K (2017) Organic-rich Albian deposits as the origin of hydrocarbon-contaminated phosphates, southeastern Constantine Basin, Algeria. J Petrol Sci Eng 157:680–695

Bismuth H, Boltenhagen C, Donze P, Le Fevre J, Saint-Marc P (1981) Le Crétacé moyen et supérieur du djebel Semmama (Tunisie du Centre-Nord): microstratigraphie et évolution sédimentologique. Bull Centres Rech Explor-Prod Elf-Aquitaine 5:193–267

Bobier C, Viguier C, Chaari A, Chine A (1991) The post-Triassic sedimentary cover of Tunisia: seismic sequences and structure. Tectonophysics 195:371–410

Bouaziz S, Barrier E, Soussi M, Turki M, Zouari H (2002) Tectonic evolution of the northern African margin in Tunisia

from paleostress data and sedimentary record. Tectonophysics 357:227–253
Briggs DEG, Kear AJ, Martill DM, Wilby PR (1993) Phosphatization of soft-tissue in experiments and fossils. J Geol Soc London 150:1035–1038
Burollet PF (1956) Contribution à l'étude stratigraphique de la Tunisie Centrale. Ann Mines Géol 18:350
Burollet PF, Memmi L, M'Rabet A (1983) Le Crétacé inférieur de Tunisie. Aperçu stratigraphique et sédimentologique Zitteliana 10:255–264
Busson G (1972) Principes, méthodes et résultats d'une étude stratigraphique du Mésozoïque saharien : Mém Museum Nation Hist Natur, Paris. Série C 26:441
Castany G (1951) Etude géologique de l'Atlas tunisien oriental. Annales Mines Géol 8:632
Cattaneo A, Steel RJ (2003) Transgressive deposits: a review of their variability. Earth Sci Rev 62:187–228
Chihaoui A (2009) La transgression albienne dans la région de Tajerouine en Tunisie centrale: Stratigraphie, sédimentologie et tectonique synsédimentaire. PhD Thesis Univ Grenoble-Sfax, p 289. https://tel.archives-ouvertes.fr/search/index/?q=Chihaoui&submitType_s=file&docType_s=THESE&authIdHal_s=abir-chihaoui
Chihaoui A, Jaillard E, Latil J-L, Susperregui A-S, Touir J, Ouali J (2010) Stratigraphy of the Hameima and lower Fahdene formations in the Tajerouine area (Northern Tunisia). J Afr Earth Sci 58:387–399
Compton JS, Bergh EW (2016) Phosphorite deposits on the Namibian shelf. Marine Geol 380:290–314
Dubourdieu G (1956) Etude géologique de la région de l'Ouenza (confins Algéro-tunisiens): Publ Serv Carte Géol Algérie 10: 659
El Euchi H (1993) La Tunisie du Centre-Ouest de l'Aptien à l'Actuel: Tectonique coulissante, dynamique sédimentaire associée et évolution du champ de contraintes Mio-Plio-Quaternaire. PhD Thesis Univ Tunis II, 261 p.
El Rabia A, Inoubli MH, Ouaja M, Abidi O, Sebei K, Jlailia A (2018) Salt tectonics and its effect on the structural and sedimentary evolution of the Jeffara Basin, Southern Tunisia. Tectonophysics 744:350–372
Emery D, Myers KJ (1996) Sequence stratigraphy. Blackwell, Oxford, p 297
Fabre J (2005) Le Mésozoïque. Géologie du Sahara occidental et central. Trevuren Afri Géosci Collect 108:361–415 ((**Musée Royal Afrique centrale, Belgium**))
Föllmi KB (1996) The phosphorus cycle, phosphogenesis and marine phosphate-rich deposits. Earth-Sci Rev 40:55–124
Föllmi KB (2016) Sedimentary condensation. Earth-Sci Rev 152:143–180
Gabtni H, Jallouli C, Mickus KI, Dhaoui M, Moncef Turki M, Jaffal M, Keating P (2012) Basement structure of southern Tunisia as determined from the analysis of gravity data: implications for petroleum exploration. Petrol Geosci 18:143–152
Ghanmi MA, Barhoumi A, Ghanmi M, Zargouni F (2017) Aptian-Albian boundary in Central Southern Atlas of Tunisia: New tectono-sedimentary facts. J Afr Earth Sci 132:27–36
Gharbi M, Espurt N, Masrouhi A, Bellier O, Amari EA (2015) Style of Atlassic tectonic deformation and geodynamic evolution of the southern Tethyan margin, Tunisia. Marine Petrol Geol 66:801–816
Hancock JM, Kaufmann EG (1979) The great transgression of the late Cretaceous. J geol Soc Lond 136:175–186
Haq BU (2014) Cretaceous eustasy revisited. Global Planet Change 113:44–58
Hays JD, Pitman WC III (1973) Lithospheric plate motion, sea level changes and climatic and ecological consequences. Nature 246:18–22
Heldt M, Lehmann J, Bachmann M, Negra MH, Kuss J (2010) Increased terrigenous influx but no drowning: palaeoenvironmental evolution of the Tunisian carbonate platform margin during the Late Aptian. Sedimentology 57:695–719
Henderson RA (2004) A mid-Cretaceous association of shell beds and organic-rich shale: bivalve exploitation of a nutrient-rich, anoxic sea-floor environment. Palaios 19:156–169
Hendry JP, Pearson MJ, Trewin NH, Fallick AE (2006) Jurassic septarian concretions from NW Scotland record interdependent bacterial, physical and chemical processes of marine mudrock diagenesis. Sedimentology 53:537–565
Hfaiedh R, Arnaud Vanneau A, Godet A, Arnaud H, Zghal I, Ouali J, Latil J-L, Jallali H (2013) Biostratigraphy, palaeoenvironments and sequence stratigraphy of the Aptian sedimentary succession at Jebel Bir Oum Ali (Northern Chain of Chotts, South Tunisia): comparison with contemporaneous Tethyan series. Cretac Res 46:177–207
Houla Y, Hanini A, Zagrarni MF, Trabelsi K, Bahrouni N, Nasri A, Ferhi F, Soussi M, Maamri R (2017) Découverte d'une série margino-littorale à continentale apto-albienne à charophytes en Tunisie centro-meridionale (Jebel Majoura): caractérisations sédimentologique, paléontologique et paléogéographique. Annales Mines Géol Tunisie 47:68–79
Hwang I-G, Heller PL (2002) Anatomy of a transgressive lag: Panther Tongue Sandstone, Star Point Formation, central Utah. Sedimentology 49:977–999
Jaillard E, Latil J-L, Chiahoui A, Zghal I (2005) Albian sedimentation in the Tadjerouine area: field guide-book, Aptian-Turonian events in Central Tunisia. Géol Alpine, sér Coll Excurs 5:105–124
Jaillard E, Bouillin J-P, Ouali J, Dumont T, Latil J-L, Chihaoui A, Zghal I (2013) The "Albian Crisis" in Central Tunisia: nature and chronology of the deformations. J Afr Earth Sci 85:75–86
Jaillard E, Bouillin J-P, Ouali J, Dumont T, Latil J-L, Chihaoui A (2017) Albian deformation in Central Tunisia: evidences for an Atlantic-type passive margin. J Afr Earth Sci 135:220–234
Kennedy WJ, Gale AS, Bown PR, Caron M, Davey RJ, Gröcke D, Wray DS (2000) Integrated stratigraphy across the Aptian-Albian boundary in the Marnes Bleues, at the Col de Pré-Guittard, Arnayon (Drôme), and at Tartonne (Alpes-de-Haute-Provence), France: a candidate Global Boundary Stratotype Section and Boundary Point for the base of the Albian Stage. Cretac Res 21:591–720
Kennedy JW, Gale AS, Huber BT, Petrizzo MR, Bown P, Jenkyns HC (2017) The Global Boundary Stratotype Section and Point (GSSP) for the base of the Albian Stage, of the Cretaceous, the Col de Pré-Guittard section, Arnayon, Drôme, France. Episodes 40:177–188
Khalifa Z, Affouri H, Rigane A, Jacob J (2018) The Albian oceanic anoxic events record in central and northern Tunisia: Geochemical data and paleotectonic controls. Marine Petrol Geol 93:145–165
Krimi M, Ouaja M, Zargouni F (2017) Upper Albian to Lower Turonian deposits and associated breccias along the Dahar cuestas (southeastern Tunisia): origin and depositional environments. J Afr Earth Sci 135:140–151
Lamboy M (1990) Microbial mediation in phosphatogenesis: new data from the Cretaceous phosphatic chalks of northern France. In: Notholx AJG, Jarvis I (eds) Phosphorite Research and Development. Geol Soc, Spec Publ 52:157–167
Latil J-L (2011) Lower Albian ammonites from Central Tunisia and adjacent areas of Algeria. Rev Paléobiol Genève 30:321–429
Layeb M, Ben Fadhel M, Ben Youssef M (2012) Thrombolitic and coral buildups in the Upper Albian of the Fahdene basin (North Tunisia): stratigraphy, sedimentology and genesis. Bull Soc géol France 183:217–231
Lazzez M, Zoughi T, Ben Youssef M (2008) Austrian phase on the northern African margin iferred from sequence stratigraphy and

sedimentary records in southern Tunisia (Chotts and Djeffara areas). C R Geosci 340:543–552

Lehmann J, Heldt M, Bachmann M, Negra MH (2009) Aptian (Lower Cretaceous) biostratigraphy and cephalopods from north central Tunisia. Cretac Res 30:895–910

M'Rabet A, Mejri F, Burollet PF, Memmi L, Chandoul H (1995) Catalog of Type Sections in Tunisia: cretaceous. Entreprise Tunisienne des Activités Pétrolières-ETAP Mém, pp 123

Martinez C, Chikhaoui M, Truillet R, Ouali J, Creuzot G (1991) Le contexte géodynamique de la distension albo-aptienne en Tunisie septentrionale et centrale: structuration éocrétacée de l'Atlas tunisien. Eclog Geol Helv 84:61–82

Masrouhi A, Bellier O, Ben Youssef M, Koyi H (2014) Submarine allochthonous salt sheets: gravity-driven deformation of North African Cretaceous passive margin in Tunisia–Bled Dogra case study and nearby salt structures. J Afr Earth Sci 97:125–142

Masse J-P, Thieuloy J-P (1979) Précisions sur l'âge des calcaires et des formations associées de l'Aptien sud-constantinois (Algérie). Conséquences paléogéographiques Bull Soc Géol France 7:65–71

Mort HP, Adatte T, Keller G, Bartels D, Föllmi KB, Steinmann P, Berner Z, Chellai EH (2008) Organic carbon deposition and phosphorus accumulation during Oceanic Anoxic Event 2 in Tarfaya, Morocco. Cretac Res 29:1008–1023

Moulin M, Aslanian D, Unternehr P (2010) A new starting point for the South and equatorial Atlantic Ocean. Earth Sci Rev 98:1–37

M'Rabet A (1981) Stratigraphie, sédimentation et diagenèse carbonatée des séries du Crétacé inférieur de Tunisie centrale. PhD thesis Univ Paris-Sud, pp 540

Nasri A, Trabelsi K, El Ferhi F, Skanji A, Ben Alaya S, Houla Y, Soussi M, Kadri A, Bouakadi N, Sames B, Wagreich M (2017) Aptian shallow marine carbonate platform and Lower Albian lacustrine and fan delta siliciclastic deposits of Jebel Koumine (Central Atlas Tunisia). 10th Internat Symp Cretaceous, Proceed, p. 193, Vienna

Parrish JT, Curtis RL (1982) Atmospheric circulation, upwelling, and organic-rich rocks in the Mesozoic and Cenozoic eras. Palaeogeogr Palaeoclim Palaeoecol 40:31–66

Philip J, Masse J-P, Bessais H (1989) Organisation et évolution sédimentaires d'une marge de plate-forme carbonatée: l'Albien-Cénomanien de Tunisie centrale. Géol Méditer 15:155–169

Pohl A, Laugié M, Borgomano J, Michel J, Lanteaume C, Scotese CR, Frau C, Poli E, Donnadieu Y (2019) Quantifying the paleogeographic driver of Cretaceous carbonate platform development using paleoecological niche modeling. Palaeogeogr Palaeoclim Palaeoecol 514:222–232

Puhfal PK, Groat LA (2017) Sedimentary and igneous phosphate deposits: formation and exploration. Econ Geol 112:483–516

Raiswell R, Fisher QJ (2004) Rates of carbonate cementation associated with sulphate reduction in DSDP/ODP sediments: implications for the formation of concretions. Chem Geol 211:71–85

Raulin C, Frizon de Lamotte D, Bouaziz S, Khomsi K, Mouchot N, Ruiz G, Guillocheau F (2011) Late triassic-early Jurassic block tilting along E-W faults, in southern Tunisia: new interpretation of the tebaga of medenine. J Afr Earth Sci 61:94–104

Rddad L, Jemmali N, Carranza EJM, Wälle M (2019) Organic matter and metal contents within the Cretaceous rocks of the Slata-Guern Halfaya area, North-Central Tunisia: Implication for ore genesis. Ore Geol Rev 113:103070

Robaszynski F, Hardenbol J, Caron M, Amédro F, Dupuis C, González-Donoso J-M, Linares D, Gartner S (1993) Sequence stratigraphy in a distal environment: the Cenomanian of the Kalaat Senan region (Central Tunisia). Bull Centres Rech Explor Prod Elf-Aquitaine 17:395–433

Robaszynski F, González-Donoso J-M, Linares D, Amédro F, Caron M, Dupuis C, Dhondt AV, Gartner S (2000) Le Crétacé supérieur de la région de Kalaat Senan, Tunisie centrale. Litho-biostratigraphie intégrée: zones d'ammonites, de foraminifères planctoniques et de nannofossiles du Turonien supérieur au Maastrichtien. Bull Centres Rech Explor-Prod Elf-Aquitaine 22:359–490

Robaszynski F, Amédro F, González-Donoso J-M, Linares D (2008) The Albian (Vraconnian)-cenomanian boundary at the western Tethyan margin (central Tunisia and southeastern France). Bull Soc géol France 179:245–266

Salama W, El-Kammar A, Saunders M, Morsy R, Kong C (2015) Microbial pathways and palaeoenvironmental conditions involved in the formation of phosphorite grains, Safaga District. Egypt Sediment Geol 325:41–58

Salmouna A, Cojan I, Touir J (2017) The charophytes-rich Barremian-Albian record in Jebel Ksaïra (Central Tunisia). J Afr Earth Sci 130:87–101

Smati A (1986) Les gisements de Pb-Ba et de Fe du Jebel Slata (Tunisie du Centre-Nord): Minéralisations épigénétiques dans le Crétacé néritique de la bordure d'un diapir de Trias. Gisements de Sidi Amor Ben Salem et de Slata-Fer. PhD Thesis Univ Paris VI, pp 250

Soua M (2015) Cretaceous oceanic anoxic events (OAEs) recorded in the northern margin of Africa as possible oil and gas shale potential in Tunisia: an overview. Internat Geol Rev 58:277–320

Souquet P, Peybernès B, Saadi J, Ben Youssef M, Ghanmi M, Zarbout M, Chikhaoui M, Kamoun F (1997) Séquences et cycles d'ordre 2 en régime extensive et transtensif: exemple du Crétacé inférieur de l'Atlas tunisien. Bull Soc Géol France 168:373–386

Talbi R, Lakhdar R, Smati A, Spiller R, Levey R (2019) Aptian-Albian shale oil unconventional system as registration of Cretaceous oceanic anoxic sub-events in the southern Tethys (Bir M'Cherga basin, Tunisia). J Petrol Explor Prod Technol 9:1007–1022

Tendil AJ-B, Frau C, Léonide P, Fournier F, Borgomano JR, Lanteaume C, Masse J-P, Massonnat G, Rolando J-P (2018) Platform-to-basin anatomy of a Barremian-Aptian Tethyan carbonate system: new insights into the regional to global factors controlling the stratigraphic architecture of the Urgonian Provence platform (southeast France). Cretac Res 91:382–411

Tesovic BC, Glumac B, Buckovic D (2011) Integrated biostratigraphy and carbon isotope stratigraphy of the Lower Cretaceous (Barremian to Albian) Adriatic-Dinaridic carbonate platform deposits in Istria, Croatia. Cretac Res 32:301–324

Tlatli M (1980) Etude des calcaires de l'Albo-Aptien des Djebels Serdj et Bellouta (Tunisie centrale). PhD Thesis Univ Aix-Marseille 2, pp 205

Tlig S (2015) The Upper Jurassic and Lower Cretaceous series of southern Tunisia and northwestern Libya revisited. J Afr Earth Sci 110:100–115

Touir J, Haj Ali H, Mahjoubi F, Ouali J (2015) Microstratigraphy and interpretation of the karst sedimentary fillings associated to the Aptian-Albian unconformity in Jebel Semmama (central Tunisia). J Afr Earth Sci 112:186–198

Trabelsi K, Touir J, Soulié-Märsche I, Martín-Closas M, Soussi M, Colin J-P (2010) Découverte de charophytes de l'Albien dans la Formation Kebar (Tunisie centrale): implications paléoécologiques et paléobiogéographiques. Annales Paléontol 96:117–133

Trabelsi K, Sames B, Salmouna A, Piovesan EK, Ben Rouina S, Houla Y, Touir J, Soussi M (2015) Ostracods from the marginal coastal Lower Cretaceous (Aptian) of the Central Tunisian Atlas (North Africa): paleoenvironment, biostratigraphy and paleobiogeography. Rev micropal 58:309–331

Trabucho Alexandre J, Van Gilst RI, Rodríguez-López JP, De Boer PL (2011) The sedimentary expression of oceanic anoxic event 1b in the North Atlantic. Sedimentology 58:1217–1246

Tucker ME, Wright VP (1990) Carbonate sedimentology. Blackwell Science, Oxford, p 482

Van Wagoner JC, Posamentier HW, Mitchum RM, Vail PR, Sarg JF, Loutit TS, Hardenbol J (1988) An overview of the fundamentals of sequence stratigraphy and key definitions. In: Wilgus CK, Hastings BS, Kendall CGSTC, Posamentier HW, Ross CA, Van Wagoner JC (eds) Sea-level changes—an integrated approach. SEPM Spec Publ 42:39–45

Vila J-M (1980) La chaîne alpine d'Algérie orientale et des confins algéro-tunisiens. Doct Thesis. Univ Paris 6, 665

Vila J-M, Ben Youssef M, Chikhaoui M, Ghanmi M (1995) Découverte d'Albien inférieur (marnes et calcaires à mélobésiées) et moyen (marno-calcaires à débris de Trias) au NW du Jebel Slata: vers l'abandon du modèle en champignon anté-vraconien. In : 3rd Congr Nat Sci Terre, Tunis, abstract, pp 8

Zghal I, Arnaud-Vanneau A (2005) The hameima formation. Aptian-turonian events in Central Tunisia. Field trip guidebook. Géol Alpine Série Spéc 5:101–104

Zghal I, Ben Hadjali N, Razgallah S, Bismuth H (1997) Foraminifères et ostracodes de l'Aptien-Albien du Jebel Hameima (région de Tadjerouine, Tunisie): biostratigraphie, paleoécologie. Afr Geosci Rev 4:361–372

Zouaghi T, Bédir M, Inoubli MH (2005) 2D Seismic interpretation of strike-slip faulting, salt tectonics, and Cretaceous unconformities, Atlas Mountains, central Tunisia. J Afr Earth Sci 43:464–486

Zouaghi T, Ferhi I, Bédir M, Youssef MB, Gasmi M, Inoubli MH, (2011) Analysis of Cretaceous (Aptian) strata in central Tunisia, using 2D seismic data and well logs. J Afr Earth Sci 61(1):38–61